Voting and catalytic processes with inhomogeneities

Mauro Mobilia and Ivan T. Georgiev*

*Center for Stochastic Processes in Science and Engineering, Department of Physics, Virginia Polytechnic Institute
and State University, Blacksburg, Virginia 24061-0435, USA*

We consider the dynamics of the voter model and of the monomer-monomer catalytic process in the presence of many "competing" inhomogeneities and show, through exact calculations and numerical simulations, that their presence results in a nontrivial fluctuating steady state whose properties are studied and turn out to specifically depend on the dimensionality of the system, the strength of the inhomogeneities, and their separating distances. In fact, in arbitrary dimensions, we obtain an exact (yet formal) expression of the order parameters (magnetization and concentration of adsorbed particles) in the presence of an arbitrary number n of inhomogeneities ("zealots" in the voter language) and formal similarities with *suitable electrostatic systems* are pointed out. In the nontrivial cases $n=1,2$, we explicitly compute the static and long-time properties of the order parameters and therefore capture the generic features of the systems. When $n>2$, the problems are studied through numerical simulations. In one spatial dimension, we also compute the expressions of the stationary order parameters in the completely disordered case, where n is arbitrary large. Particular attention is paid to the spatial dependence of the stationary order parameters and formal connections with electrostatics.

I. INTRODUCTION

Recently, much attention has been devoted to the field of nonequilibrium many-body stochastic processes [1]. In particular the study of exact solutions of prototypical models such as the *voter model* [2] has proved to be fruitful for understanding a broad class of nonequilibrium phenomena [1]. In modeling nonequilibrium systems, it is often assumed that the underlying spatial structure is homogeneous. However, in real situations stochastic processes take place in the presence of imperfections (dislocations, defects, etc.) that modify locally the interactions (see, e.g., [1,3] and references therein). It is therefore highly desirable to take into account the effects of disorder, inhomogeneities, and defects or other spatial constraints within simple and mathematically amenable models. Motivated by the above considerations, in a recent Letter [4], the properties of a paradigmatic nonequilibrium statistical mechanics model (the voter model) in the presence of one single inhomogeneity (a "zealot") have been studied and it was shown that the presence of single zealot has dramatic effects on the dynamics and the steady state. For this model, in low dimensions, all of the agents eventually follow the zealot. Obviously, real systems are quite complex and the case of a single defect cannot be considered as being generic. To gain some insight into more realistic situations, we present here an approach allowing us to compute exact properties, in arbitrary dimensions, of a class of stochastic many-body systems in the presence of *n competing inhomogeneities*. This study is carried out in the context of two physically relevant systems: the voter model and the monomer-monomer catalytic reaction (in the reaction-controlled limit). We consider such a study as a further contribution toward the understanding of a class of disordered

nonequilibrium many-body processes (where inhomogeneities would not be spatially fixed but would be randomly distributed). We show that the presence of "competing inhomogeneities" (in the sense of locally *perturbing* the otherwise homogeneous dynamics) generally results in a space-dependent fluctuating steady state. The amenable case where $n=2$ is analytically studied in detail and the static and long-time properties of the order parameters are obtained and their spatial dependence are computed. The situation where $n \geqslant 2$ is investigated by numerical simulations. Also, in one spatial dimension, we are able to compute the stationary order parameters in the completely disordered case (i.e., when n is arbitrary large). We therefore show how the stationary magnetization or concentration depends on the dimensionality of the system, the strength of the inhomogeneities, and their separating distances. In particular, we show that the local perturbation of the dynamics may give rise to subtle coarsening phenomena. In one and two dimensions (1D and 2D), when the density of the inhomogeneities is vanishing in the thermodynamic limit there is still coarsening in the system. Oppositely, when the density of the competing inhomogeneities is nonzero there is no coarsening, even in one and two dimensions. We obtain an exact, yet formal, expression of the order parameters (magnetization and concentration of adsorbed particles) in arbitrary dimension. In dimensions $d=2,3$ we pay special attention to the radial and polar dependence of these quantities. Also, formal similarities with *electrostatic systems* are pointed out. The organization of this work is the following: In the next section we introduce the inhomogeneous voter model. In Sec. III, we present the general mathematical setup and the formal solution of the problem. In Sec. IV, we study analytically the voter model in the presence of two "competing zealots" in one, two, and three dimensions and provide numerical results for the case where $n \geqslant 2$. In Sec. IV B, for the one-dimensional case, we also derive the expression of the static magnetization in the completely disordered situation where n is arbitrary large. Sec-

---

*Electronic address: mmobilia@vt.edu, georgiev@vt.edu

tion V is devoted to the study of the process of monomer-monomer catalysis reaction on an inhomogeneous substrate, whose mathematical formulation is very close to that of the (inhomogeneous) voter model and in Sec. VI we summarize and present our conclusions.

II. VOTER DYNAMICS IN THE PRESENCE OF COMPETING ZEALOTS

The (homogeneous) voter model is an Ising-like model where a spin ("individual"), associated with a lattice site r, can have two different "opinions" $\sigma_r = \pm 1$ [2]. The dynamics of such a system is implemented by randomly choosing one spin and changing its state to the value of one of its randomly chosen nearest neighbors. In the (homogeneous) voter model, the global magnetization is conserved and the dynamics is Z_2 symmetric (invariance under the global inversion $\sigma_r \rightarrow -\sigma_r$). The importance of the voter model stems from the fact that it is one of a very few stochastic many-body systems that are solvable in any dimension. It is useful for describing the kinetics of catalytic reactions [5,6], for studying coarsening phenomena [7,8], and also serves as a prototype model for opinion dynamics [4,9,10].

Concepts inspired by statistical mechanics have already been employed to some extent in the last two decades to mimic social issues [11]. Very recently variants of the voter model and modern tools of nonequilibrium statistical physics, such as various mean-field-like approaches and exact methods [4,12,15], numerical simulations [9,13,14,16], and formulation on random networks [10,16] (see also references therein), were used intensively to quantitatively study further, both mathematically and numerically, collective phenomena, such as the opinion formation, inspired by sociocultural situations. In this context, the voter model and its variants play a key rôle, as it is often used as a reference model. Despite of all these efforts, voterlike models have mainly be studied on homogeneous and/or translationally invariant spatial structures.

In contrast to most of the previous works, here we study, using exact analytical methods and numerical simulations, a spatially inhomogeneous voter model. It is defined on a hypercubic lattice of size $(2L+1)^d$, where individuals, labeled by a vector r having components $-L \leq r_i \leq L$ (with $i = 1, \ldots, d$), may interact according to the usual voter dynamics. In addition, we now consider that there are n zealots (labeled $j = 1, \ldots, n$), occupying the sites $\{a^j = (a_1^j, \ldots, a_d^j)\}$. These agents interact with their neighboring spins in a biased fashion. A zealot at site a^j favors one of the opinions $\epsilon_j = \pm 1$, i.e., it flips with an additional rate $\alpha_j > 0$ (additional to the usual voter rate) toward his favorite state. As the zealots interact effectively with all of the spins on the lattice, there is a competition between them aiming at "convincing" as many spins as possible. Clearly, because the zealots perturb the dynamics locally, the system is disordered, not translationally invariant and the magnetization is not conserved.

According to the spin formulation of the model, the state of the system is described by the collection of all spins: $S \equiv \{\sigma_r\}$. In this language, the dynamics of the model is governed by the usual voter model transition rate [2,5,6] supple-

mented by local terms involving the zealots' reaction. The spin-flip rate $w_r(S) \equiv w(\sigma_r \rightarrow -\sigma_r)$ therefore reads

$$w_r(S) = \frac{1}{\tau}\left(1 - \frac{1}{2d}\sigma_r\sum_{r'}\sigma_{r'}\right) + \sum_{j=1}^{n}\frac{\alpha_j}{2}(1 - \epsilon_j\sigma_{a^j})\delta_{r,a^j}. \quad (1)$$

Here the sum on right-hand side (RHS) runs over the $2d$ nearest neighbors r' of site r and $\tau \equiv 1/d > 0$ defines the time scale. The probability distribution $P(S,t)$ satisfies the master equation

$$\frac{d}{dt}P(S,t) = \sum_{r}[w_r(S^r)P(S^r,t) - w_r(S)P(S,t)], \quad (2)$$

where the state S^r differs from configuration S only by the spin flip of σ_r. Using the master equation (2), in the thermodynamic limit $L \rightarrow \infty$, the equation of motion of the local magnetization at site r, denoted by $S_r(t) \equiv \Sigma_S\sigma_r P(S,t)$, reads

$$\frac{d}{dt}S_r(t) = \Delta_r S_r(t) + \sum_{j=1}^{n}\alpha_j[\epsilon_j - S_{a^j}(t)]\delta_{r,a^j}. \quad (3)$$

Here Δ_r denotes the discrete Laplace operator: $\Delta_r S_r(t) \equiv -2dS_r(t) + \Sigma_{r'}S_{r'}(t)$. We can immediately notice from Eq. (3) that the stationary magnetization obeys a discrete Poisson-like equation $\Delta_r S_r(\infty) = \Sigma_{j=1}^{n}\alpha_j[S_{a^j}(\infty) - \epsilon_j]\delta_{r,a^j}$. There is an obvious and striking resemblance between this equation and the well-known equation for the electrostatic potential generated by n classical point charges located at $\{a^j\}$. Therefore, one may be tempted to formally identify $S_r(\infty)$ with an electrostatic potential and think that the problem could be solved easily. In fact, the problem is much harder since the quantities playing the role of charges depend themselves on the magnetization. *In other words, the problem of finding the stationary magnetization is isomorphic to the problem of determining the electrostatic potential in a discrete system where the value of the charges depend on the potential itself.* Because of this fact, the calculation of $S_r(\infty)$ cannot be inferred directly from the results known from electrostatics and the computations have to be carried out in a self-consistent manner, as described hereafter.

III. GENERAL SETUP AND FORMAL SOLUTION

In this section, we show how to compute the magnetization of the voter model in the presence of an arbitrary number of inhomogeneities (competing zealots) and provide a "formal" solution of Eq. (3).

For further use, we introduce the following quantity: $\hat{I}_r(s) \equiv \int_0^{\infty}dt e^{-st}[e^{-2dt}I_{r_1}(2t)\cdots I_{r_d}(2t)] = \hat{I}_{-r}(s)$, where $I_n(2t) = I_{-n}(2t) = \int_0^{\pi}(dq/\pi)\cos(qn)e^{2t\cos q}$ is the usual modified Bessel function of the first kind [20]. The quantity $\hat{I}_r(s)$ can be rewritten in terms of Watson integrals or "lattice Green functions":

$$\hat{I}_r(s) = \hat{I}_{-r}(s) = \int_{-\pi}^{\pi}\frac{d^dq}{(2\pi)^d}\frac{e^{-iq\cdot r}}{s + 2\left[d - \sum_{i=1}^{d}\cos q_i\right]}, \quad (4)$$

where $q = (q_1, \ldots, q_d)$ is a d-dimensional vector. We also introduce the Fourier transform of the magnetization

$$\mathcal{S}_q(t) = \sum_r e^{iq\cdot r} S_r(t). \tag{5}$$

Fourier transforming Eq. (3), we obtain the following equation:

$$\frac{d}{dt}\mathcal{S}_q(t) = -2d\left(1 - \frac{1}{d}\sum_{i=1}^{d}\cos q_i\right)\mathcal{S}_q(t) + \sum_{j=1}^{n}e^{iq\cdot a^j}A^j(t),\tag{6}$$

where $A^j(t) \equiv \alpha_j[\epsilon_j - S_{a^j}(t)]$. Laplace-transforming Eq. (6), we obtain the following expression for the Laplace-Fourier transform of the magnetization:

$$\hat{\mathcal{S}}_q(s) = \frac{\sum_j e^{iq\cdot a^j}\hat{A}^j(s)}{s + 2d\left\{1 - \frac{1}{d}\sum_{i=1}^{d}\cos q_i\right\}},\tag{7}$$

where $\hat{A}^j(s) \equiv \int_0^\infty dt e^{-st}A^j(t)$. For technical simplicity, we have considered that the system is initially in a state with zero magnetization: $S_r(0)=0$. Inverse-Fourier-transforming Eq. (7), we get the Laplace transform $\hat{S}_r(s)$ of the magnetization:

$$\hat{S}_r(s) = \sum_\ell \int_{-\pi}^{\pi}\frac{d^dq}{(2\pi)^d}\frac{\hat{A}^\ell(s)e^{i(a^\ell-r)\cdot q}}{s + 2d\left\{1 - \frac{1}{d}\sum_{i=1}^{d}\cos q_i\right\}}.\tag{8}$$

As both right- and left-hand sides still depend on the Laplace transform of the magnetization [through $\hat{A}^j(s)$ on the RHS], to obtain an explicit expression for $\hat{S}_{a^j}(s)$, we have to find a self-consistent solution of Eq. (8) for all of the a^j's by plugging $r=a^j$ into Eq. (8). Solving the resulting linear system, in thermodynamic limit ($L\rightarrow\infty$) we obtain

$$\hat{S}_{a^j}(s) = \sum_\ell \int_{-\pi}^{\pi}\frac{d^dq}{(2\pi)^d}\frac{\hat{A}^\ell(s)e^{i(a^\ell-a^j)\cdot q}}{s + 2d\left\{1 - \frac{1}{d}\sum_{i=1}^{d}\cos q_i\right\}},\tag{9}$$

which can be rewritten $\sum_\ell(\mathcal{M}_{j,\ell} + \delta_{j,\ell}/\alpha_j)\hat{A}^\ell(s) = \epsilon_j/s$, where the symmetric $n\times n$ matrix $\mathcal{M}$ is defined as follows:

$$\mathcal{M}_{j,\ell}(s) = \int_{-\pi}^{\pi}\frac{d^dq}{(2\pi)^d}\frac{e^{i(a^\ell-a^j)\cdot q}}{s + 2d\left\{1 - \frac{1}{d}\sum_{i=1}^{d}\cos q_i\right\}}$$

$$= \hat{I}_{a^j-a^\ell}(s) = \hat{I}_{a^\ell-a^j}(s).\tag{10}$$

To obtain the two last equalities, we used the integral representation (4). We now introduce another symmetric $n\times n$ matrix $\mathcal{N}$ defined by

$$\mathcal{N}_{j,\ell}(s,\{\alpha\}) \equiv \mathcal{M}_{j,\ell}(s) + \frac{\delta_{j,\ell}}{\alpha_j},\tag{11}$$

and from it, using Eq. (9), one obtains $\hat{A}^j$ and $\hat{S}_{a^j}$:

$$\hat{A}^j(s) = \frac{1}{s}\sum_\ell \epsilon_\ell[\mathcal{N}^{-1}(s,\{\alpha\})]_{j,\ell},\tag{12}$$

$$\hat{S}_{a^j}(s) = \frac{1}{s}\left(\epsilon_j - \frac{1}{\alpha_j}\sum_\ell \epsilon_\ell[\mathcal{N}^{-1}(s,\{\alpha\})]_{j,\ell}\right).\tag{13}$$

At this point, we can get an explicit expression for the Laplace transform of the magnetization by plugging back Eq. (12) into Eq. (8). In the thermodynamic limit ($L\rightarrow\infty$), we have

$$\hat{S}_r(s) = \frac{1}{s}\sum_{j,\ell}\epsilon_\ell\hat{I}_{a^j-r}(s)[\mathcal{N}^{-1}(s,\{\alpha\})]_{j,\ell},\tag{14}$$

and therefore, formally the magnetization is obtained by Laplace-inverting Eq. (14):

$$S_r(t) = \frac{1}{2\pi i}\int_{c-i\infty}^{c+i\infty}\frac{ds}{s}e^{st}\sum_{j,\ell}\epsilon_\ell\hat{I}_{a^j-r}(s)[\mathcal{N}^{-1}(s,\{\alpha\})]_{j,\ell}.\tag{15}$$

This expression means that we have recast the problem of solving the inhomogeneous voter model in the presence of arbitrary many inhomogeneities into a well-defined linear algebra problem whose main, but nontrivial, analytic difficulty resides in the inversion of the matrix $\mathcal{N}$. The steady state of the magnetization for $L\rightarrow\infty$ can be directly inferred from Eq. (14) as follows:

$$S_r(\infty) = \lim_{s\rightarrow 0}\sum_{j,\ell}\epsilon_\ell\hat{I}_{a^j-r}(s)[\mathcal{N}^{-1}(s,\{\alpha\})]_{j,\ell}.\tag{16}$$

The exact expression for the long-time magnetization is obtained by Laplace-inverting the $s\rightarrow 0$ expansion of Eq. (14), after having subtracted the static contribution $S_r(\infty)/s$, and by paying due attention to the situations where the integrals (4) are divergent. It is also worth mentioning that the properties of the modified Bessel functions of the first kind, $I_r(t)$ [20], allow us to write a formal and implicit solution of Eq. (3) for $L\rightarrow\infty$, which reads

$$S_r(t) = \sum_k S_k(0)\prod_{i=1}^{d}[e^{-2t}I_{k_i-r_i}(2t)]$$

$$+ \sum_j \alpha_j\int_0^t dt' A^j(t-t')\prod_{i=1}^{d}[e^{-2t'}I_{r_i-a_i^j}(2t')].\tag{17}$$

To solve it explicitly for $S_r(t)$, one has to Laplace-transform Eq. (17) and then solve the resulting linear system [4], which is equivalent to the procedure described above. Expression (17) is advantageous if one is interested in the global magnetization of the system. In fact, as we consider an initially homogeneous and "neutral" system [$S_k(0)=0$], using Eq. (17), the global magnetization of the system can be written

$$M(t) \equiv \sum_{\mathbf{k}} S_{\mathbf{k}}(t) = \sum_{j=1}^{n} \int_0^t d\tau A^j(\tau) = \sum_{j=1}^{n} \alpha_j \int_0^t d\tau [\epsilon_j - S_{\mathbf{a}^j}(\tau)], \quad (18)$$

where we use the identity $\Sigma_{k=-\infty}^{\infty} I_k(t) = e^t$ [20].

The situation considered here is particularly interesting when the zealots favor different opinions and there is an effective competition occurring in the system. In this case we expect nontrivial nonequilibrium space-dependent steady states. Of course, we can easily check that in the presence of one single zealot ($n=1$) located at site **0**, with strength $\alpha_1 = \alpha$ and $\epsilon_1 = 1$, we recover the results reported in Ref. [4]. In this case we simply have $\mathcal{N}^{-1} = \alpha[\alpha\hat{I}_{\mathbf{0}}(s) + 1]^{-1}$ and, together with Eq. (8), we recover $\hat{S}_{\mathbf{r}}(s) = \alpha\hat{I}_{\mathbf{r}}(s)/s[\alpha\hat{I}_{\mathbf{0}}(s) + 1]$. In Ref. [4], one of us has shown that in low dimensions the voter

model with only one zealot evolves toward the unanimous state favored by the inhomogeneity.

IV. VOTER MODEL IN THE PRESENCE OF TWO COMPETING ZEALOTS

In this section we specifically consider the case where two competing zealots are present ($j=1,2$): One, with strength $\alpha_1 = \alpha$, located at site $\mathbf{a}^1 = \mathbf{0}$ and the other located at site $\mathbf{a}^2 = \mathbf{x}$ with a strength $\alpha_2 = \beta$. This case is explicitly tractable and displays interesting features, which turns out to be generic for the case $n > 1$ as illustrated by numerical simulations. For this case, we have

$$\mathcal{N} = \begin{pmatrix} \hat{I}_0(s) + \alpha^{-1} & \hat{I}_x(s) \\ \hat{I}_x(s) & \hat{I}_0(s) + \beta^{-1} \end{pmatrix}$$

for $L \to \infty$, and therefore, using Eq. (14), we infer the expression of the Laplace transform of the magnetization at site $\mathbf{r}$:

$$\hat{S}_{\mathbf{r}}(s) = \frac{1}{s} \sum_{j,\ell} \hat{I}_{\mathbf{a}^j - \mathbf{r}}(s)\epsilon_\ell(s)[\mathcal{N}^{-1}(s,\{\alpha\})]_{j,\ell} = \frac{\alpha\epsilon_1\hat{I}_{\mathbf{r}}(s) + \beta\epsilon_2\hat{I}_{\mathbf{r}-\mathbf{x}}(s) + \alpha\beta\{\hat{I}_{\mathbf{r}}(s)[\epsilon_1\hat{I}_{\mathbf{0}}(s) - \epsilon_2\hat{I}_{\mathbf{x}}(s)] + \hat{I}_{\mathbf{r}-\mathbf{x}}(s)[\epsilon_2\hat{I}_{\mathbf{0}}(s) - \epsilon_1\hat{I}_{\mathbf{x}}(s)]\}}{s\{1 + (\alpha + \beta)\hat{I}_{\mathbf{0}}(s) + \alpha\beta[\hat{I}_{\mathbf{0}}^2(s) - \hat{I}_{\mathbf{x}}^2(s)]\}}, \quad (19)$$

where $\epsilon_{1,2} = \pm 1$. Obviously, the inhomogeneous system with two zealots is interesting in the case when $\epsilon_1 = -\epsilon_2$. In fact, it is clear from Ref. [4] that in 1D and 2D the condition $\epsilon_1 = \epsilon_2$ implies that $S_{\mathbf{r}}(\infty) = \epsilon_1$. In this situation, the long-time approach toward the unanimous steady state is $S_{\mathbf{r}}(t) - S_{\mathbf{r}}(\infty) \simeq \mathcal{A}t^{-1/2}$ in one dimension and $S_{\mathbf{r}}(t) - S_{\mathbf{r}}(\infty) \simeq \mathcal{B}/\ln t$ in two dimensions. Thus, in low dimensions, when $\epsilon_1 = \epsilon_2$, only the long-time amplitudes $\mathcal{A}$ and $\mathcal{B}$ change with respect to the case where $n=1$ and $\epsilon = \epsilon_1$ [4].

From now on, without loss of generality, we consider the more interesting situation when there is a competition between the zealots: $\epsilon_1 = -\epsilon_2 = 1$. Namely, the zealot at the origin favors the +1 opinion, whereas the zealot at site $\mathbf{x}$ favors the opposite −1 state. In this case, Eq. (19) simplifies as follows:

$$\hat{S}_{\mathbf{r}}(s) = \frac{\alpha\hat{I}_{\mathbf{r}}(s) - \beta\hat{I}_{\mathbf{r}-\mathbf{x}}(s) + \alpha\beta[\hat{I}_{\mathbf{r}}(s) - \hat{I}_{\mathbf{r}-\mathbf{x}}(s)][\hat{I}_{\mathbf{0}}(s) + \hat{I}_{\mathbf{x}}(s)]}{s\{1 + (\alpha + \beta)\hat{I}_{\mathbf{0}}(s) + \alpha\beta[\hat{I}_{\mathbf{0}}^2(s) - \hat{I}_{\mathbf{x}}^2(s)]\}}. \quad (20)$$

Different questions can be asked here: What is the range of influence of each zealot? How "efficient" are the zealots? How does the opinion of a randomly picked spin evolve with the time, and what will be its final opinion? These questions will be answered in the next sections by explicit calculation of the stationary magnetization and its long-time behavior.

A. Results in 1D

First we focus on the one-dimensional situation and consider the case when both competing zealots are separated by

a *finite* distance x [see Fig. 1(a)]. It is worth studying the properties of the one-dimensional version of the inhomogeneous voter model because of its physical implication for the catalysis (see Sec. V) and its close relationship with the Ising model with Glauber dynamics, which is an important theoretical model, known to have many physical applications [1,4]. In fact, in the absence of zealots the one-dimensional voter model coincides with the Glauber-Ising model with zero temperature dynamics [17,18].

In 1D, one computes explicitly $\hat{I}_{\mathbf{r}}(s)$ in Eq. (4) as follows [20,21]:

$$\hat{I}_{\mathbf{r}}(s) \equiv \hat{I}_r(s) = \frac{\{[\sqrt{s+4} - \sqrt{s}]/2\}^{2r}}{\sqrt{s(s+4)}}, \quad (21)$$

where $r = |\mathbf{r}|$. We see that, in 1D, $\hat{I}_r(s)$ diverges for small s as $s^{-1/2}$.

Without loss of generality we consider the situation illustrated in Fig. 1 and thus, from Eqs. (20) and (21), the long-time expression for $S_r(t)$ in the case where $r \in [0, x]$ is

$$S_r(t) = \left(\frac{\alpha - \beta - \alpha\beta(2r - x)}{\alpha + \beta + \alpha\beta x} \right) - \frac{1}{(\alpha + \beta + \alpha\beta x)\sqrt{\pi t}}$$

$$\times \left[\frac{2\{\alpha - \beta - \alpha\beta(2r - x)\} + \alpha\beta x\{\beta(x - r) - r\alpha\}}{\alpha + \beta + \alpha\beta x} \right.$$

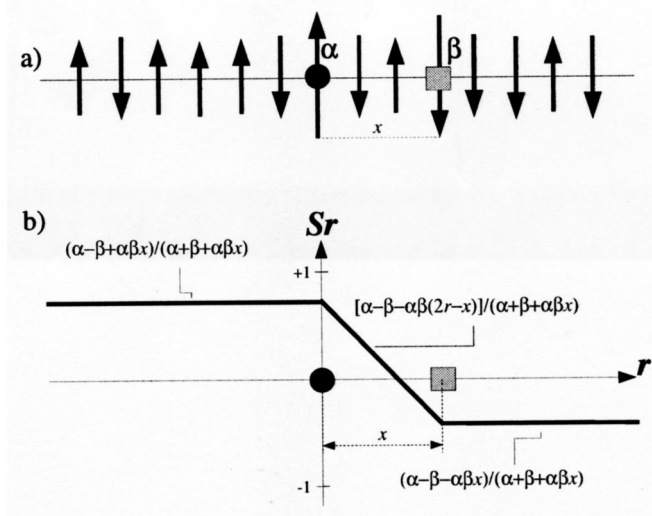$$\left. + \alpha r + \beta(r - x) \right]. \quad (22)$$

FIG. 1. (a) Graphical representation of a microscopic configuration of the spins on a one-dimensional chain. The zealot favoring the +1 opinion with a strength α, indicated by a dot and a larger up spin, is at the origin. On the right of the origin, at a distance x, the other zealot, indicated by a square and a larger down spin, favors the −1 state with a strength β. (b) Typical 1D stationary magnetization profile $S_r(\infty)$ (denoted simply S_r in the figure) versus r in the thermodynamic limit. On the left of the origin and the right of the other zealot, the static magnetization reaches two plateaus with heights given by Eqs. (23) and (24). Between the zealots, the stationary magnetization varies linearly according to Eq. (22).

For the spins on the right of the origin, with $x < r < \infty$, we find

$$S_r(t) = \left(\frac{\alpha - \beta - \alpha\beta x}{\alpha + \beta + \alpha\beta x} \right) - \frac{1}{(\alpha + \beta + \alpha\beta x)\sqrt{\pi t}}$$
$$\times \left[\frac{2(\alpha - \beta - \alpha\beta x) - \alpha^2\beta x^2}{\alpha + \beta + \alpha\beta x} + \alpha r + \beta(x - r) \right], \quad (23)$$

whereas for the spins on the left of the origin, with $0 < r < \infty$, we find

$$S_{-r}(t) = \left(\frac{\alpha - \beta + \alpha\beta x}{\alpha + \beta + \alpha\beta x} \right) - \frac{1}{(\alpha + \beta + \alpha\beta x)\sqrt{\pi t}}$$
$$\times \left[\frac{2(\alpha - \beta + \alpha\beta x) + \alpha\beta^2 x^2}{\alpha + \beta + \alpha\beta x} + \alpha r - \beta(r + x) \right]. \quad (24)$$

Finally, when both $r \to \infty$ and $t \to \infty$, $\hat{I}_r(s) \to e^{-r\sqrt{s}}/(2\sqrt{s})$. Using this expression in Eq. (20), as in Ref. [4], we obtain a scaling expression for the magnetization:

$$S_{\pm r}(t) \simeq \left(\frac{\alpha - \beta \mp \alpha\beta x}{\alpha + \beta + \alpha\beta x} \right) \mathrm{erfc}\left(\frac{r}{2\sqrt{t}} \right), \quad (25)$$

where $\mathrm{erfc}(x) = 2\int_x^\infty (dy/\sqrt{\pi})e^{-y^2}$ is the usual complementary error function. We infer from Eq. (22) that in the finite interval separating the two zealots, the stationary magnetization
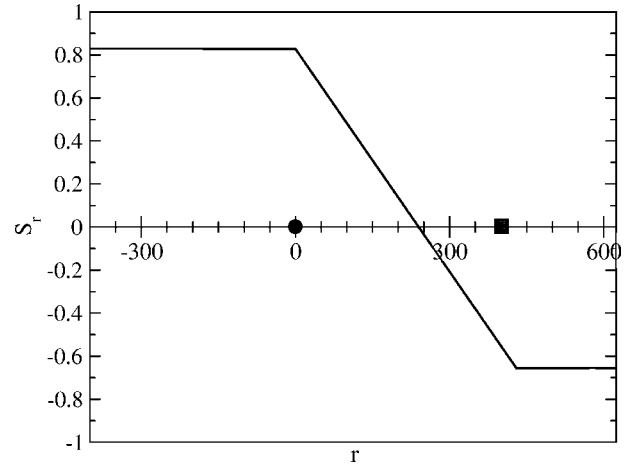

FIG. 2. The stationary distribution $S_r(\infty)$ on a $L = 1024$ lattice with two competing zealots. The zealot favoring the positive opinion (dot) is located at the origin with $\alpha = 0.02$ and the other one favoring the negative opinion (square) is at $r = 430$ with $\beta = 0.01$. The agreement with the theoretical results for an infinite system is excellent.

profile decays linearly with a slope $-2\alpha\beta/(\alpha + \beta + \alpha\beta x)$. Outside from this interval, the final magnetization is uniform on the right and left hand side from both inhomogeneities. In fact, Eqs. (23) and (24) show that the static magnetization of the spins is $S_{\pm r}(\infty) = (\alpha - \beta \mp \alpha\beta x)/(\alpha + \beta + \alpha\beta x)$ [see Figs. 1(b) and 2]. These plateaus differ significantly from the values ∓ 1 only when the product $\alpha\beta$ is comparable to x^{-1}. Therefore, in 1D, the final stationary solution, which is summarized on Fig. 1(b), is *polarized* and can be understood as being the solution of a discrete one-dimensional electrostatic Poisson equation with peculiar boundary conditions. In fact, it is well known that in 1D the electrostatic potential varies linearly with the distance to the charges. Here, the nontrivial part of the analysis is to compute in a self-consistent manner the heights of the plateaus. All these profiles are approached algebraically in time—i.e., $S_r(t) - S_r(\infty) \simeq At^{-1/2}$ (as in the case with only one zealot [4]), with the amplitude depending nontrivially of all parameters of the system $A = \widetilde{A}(\alpha, \beta, x)r$. Obviously, because there is a distance x separating the zealot at the origin from the other, the expression for $S_r(t)$ is not symmetric with respect to the site 0. We can notice that the expressions (22)–(24) simplify when the strength of the zealot is infinite ($\alpha = \beta = \infty$). In this case, the zealots have a final magnetization $S_0(\infty) = -S_x(\infty) = 1$.

Result (25) tells us that for spins *infinitely* far away from the zealots, the magnetization evolves as a smooth scaling function of the variable $u \equiv r/2\sqrt{t}$. This scaling function differs from zero (the initial condition) after a long time (i.e., $t \sim r^2 \to \infty$), when the variable u has a finite value. It follows from Eqs. (23)–(25) that in 1D the effect of the zealots is felt and propagates as $t^{1/2} \to \infty$. For large time and distance, when $1 \ll t \ll r^2$, we see from Eq. (25) that $S_r(t)$ is still close to its initial value. When $t \sim r^2$, all the agents approach as $t^{-1/2}$ the active and fluctuating stationary magnetization (23). From Eqs. (22) and (18), we can infer the long-time behavior of the global magnetization in the system. As

$$\alpha[1 - S_0(t)] - \beta[1 + S_x(t)] \simeq \frac{2(\alpha - \beta)}{\alpha + \beta + \alpha\beta x} \frac{1}{\sqrt{\pi t}},$$

when $\alpha \neq \beta$, the average number of voters following the strongest zealot evolves (at long-time) as the square root of time:

$$M(t) \simeq \frac{4(\alpha - \beta)}{\alpha + \beta + \alpha\beta x} \sqrt{\frac{t}{\pi}}.$$

This result implies that the time T necessary for the strongest zealot to dominate (on average) the whole 1D system scales as $T \sim L^2$, where $L \to \infty$. When $\alpha = \beta$, the system is exactly symmetric with respect to $x/2$, and on average there are as many +1 spins than −1 ones in the whole system.

In Fig. 2 we show the stationary magnetization $S_r(\infty)$ on a finite lattice with $L = 1024$ for two competing zealots obtained from Monte Carlo simulations. For simulating the model we use random sequential dynamics by picking randomly an "active" site (either one of the zealots or a site that has at least one nearest neighbor in a different state) and flipping it with a rate given by Eq. (1). The time after an attempt for a flip is updated with the amount $1/N_a$, where N_a is the number of active sites before the current update. To account for the fact that the simulations are on a finite lattice, where the spin at the left (right) boundary site has only one nearest neighbor on the right (left), the spin-flip rate at the boundaries is modified such that it depends only on the state of a single neighbor. The first 2×10^8 Monte Carlo steps (MCS) are discarded and typically we sample the configurations on the lattice every 5000 MCS for the next 5×10^9 MCS. The stationary distribution for $S_r(\infty)$ obtained from the simulations is in an excellent agreement with the theoretical values obtained for a infinite lattice and sketched on Fig. 1(b).

Figure 3 shows the result from Monte Carlo simulations on a relatively small ($L = 8192$) lattice for various average quantities. The long-time behavior of the local magnetization $\delta S_0(t) \equiv S_0(\infty) - S_0(t)$ and $\delta S_x(t) \equiv S_x(\infty) - S_x(t)$ clearly shows the $t^{-1/2}$ long-time behavior, in agreement with Eq. (22). In Fig. 3 we also report numerical results for the average number of interfaces (i.e., two neighboring sites with different spins) versus time. This quantity gives us a good qualitative and quantitative picture of the coarsening of the system. Figure 3 shows that the average value of the interfaces, which equals to the number of the clusters of +1 and −1 spins, evolves as $t^{-1/2}$ before saturating at a small nonzero value. One can notice that for a long time the system evolves and *coarsens* as in the homogeneous voter model [6], but due to the presence of the two competing zealots, subtleties appear at long times. In fact, one has to distinguish between the three possible situations for the coarsening: (i) when we have $n < 2$ (i.e., none or only one zealot on the lattice), there is the usual coarsening (an infinite domain spans the entire system) [6]; (ii) when $2 \leq n$ and the density (n/L) of the competing inhomogeneities is zero for $L \to \infty$, there is still coarsening in the sense that the size of the different domains formed increases with the size of the lattice but never spans the entire lattice; (iii) when the density of the competing zealots has a
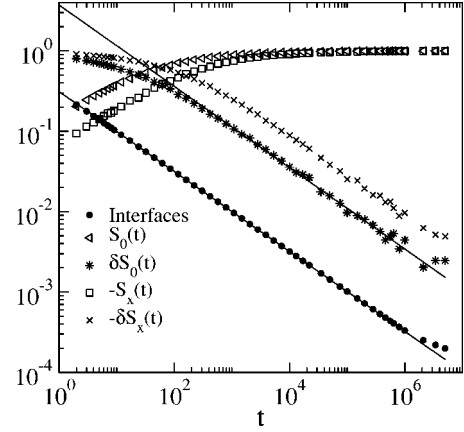

FIG. 3. Coarsening on the one-dimensional model with two competing zealots. The figure shows the average number of interfaces vs time, the average magnetization of the two zealots (see the text) $S_0(t)$ and $S_x(t)$, and also $\delta S_0(t) \equiv S_0(\infty) - S_0(t)$ and $\delta S_x(t) \equiv S_x(\infty) - S_x(t)$. The simulation is on $L = 8192$ lattice for $\alpha = 0.5$, $\beta = 0.2$, and $x = 3000$ and the solid lines shown have a slope −0.5, as predicted by Eq. (22). For this choice of the parameters, the average number of interfaces decays algebraically toward a small but finite value (here, $\approx 2.0 \times 10^{-4}$).

nonzero value in the thermodynamic limit, there is no longer coarsening as the formation of large domains is prevented by the interaction with the numerous (competing) inhomogeneities.

After having discussed in detail the case $n = 2$, we would like to point out that in one spatial dimension it is possible to compute the stationary magnetization for an arbitrary number n of zealots in a more direct and intuitive fashion than relying on Eq. (16). In fact, let us consider that the zealots, labeled by $j = 1, \ldots, n$ are at sites $-\infty < a_1 < a_2 < \cdots < a_n < \infty$. By plugging the ansatz that the stationary magnetization between the sites a^j and a^{j+1} reads $S_r(\infty) = S_{a^j}(\infty) + \gamma_j(r - a^j)$ into $\Delta_r S_r(\infty) = -\Sigma_{j=1}^n \alpha_j [\epsilon_j - S_{a^j}(\infty)] \delta_{r,a^j}$, where we have introduced $\gamma_j \equiv [S_{a^{j+1}}(\infty) - S_{a^j}(\infty)]/x_j$ and $x_j \equiv a^{j+1} - a^j$, we obtain

$$\gamma_1 \delta_{r,a_1} + (\gamma_2 - \gamma_1)\delta_{r,a_2} + \cdots + (\gamma_{n-1} - \gamma_{n-2})\delta_{r,a_{n-1}} - \gamma_n \delta_{r,a_n}$$

$$= \sum_{j=1}^n \alpha_j [S_{a^j}(\infty) - \epsilon_j] \delta_{r,a^j}. \tag{26}$$

Solving these equations, we obtain the stationary magnetization at each sites $a^1 \leq a^j \leq a^n$:

$$S_{a^1}(\infty) = \epsilon_1 + \frac{\gamma_1}{\alpha_1},$$

$$S_{a^2}(\infty) = \epsilon_2 + \frac{\gamma_2 - \gamma_1}{\alpha_2},$$

$$\vdots \quad \vdots \quad \vdots$$

$$S_{a^{n-1}}(\infty) = \epsilon_{n-1} + \frac{\gamma_{n-1} - \gamma_{n-2}}{\alpha_{n-1}},$$

$$S_{a^n}(\infty) = \epsilon_n - \frac{\gamma_{n-1}}{\alpha_n}. \qquad (27)$$

Of course, in each of these equations for $S_{a^j}(\infty)$, the right-hand side depends on $S_{a^j}(\infty)$ and $S_{a^{j+1}}(\infty)$ through γ_j. Equations (27) are therefore a set of coupled linear equations that can be rewritten as $PS = v$, where P is a $n \times n$ band matrix, which only nonvanishing entries are

$$P_{j,j} = -(x_{j-1} + x_j + \alpha_j x_{j-1} x_j), \quad 1 < j < n,$$

$$P_{j,j-1} = x_j, \quad 1 < j < n,$$

$$P_{j,j+1} = x_{j-1}, \quad 1 < j < n,$$

$$P_{1,1} = -(1 + \alpha_1 x_1),$$

$$P_{n,n} = -(1 + \alpha_n x_{n-1}),$$

$$P_{1,2} = P_{n,n-1} = 1, \qquad (28)$$

and S and v are column vectors which components are, respectively,

$$S_j = S_{a^j}(\infty), \quad 1 \leq j \leq n,$$

$$v_1 = -\epsilon_1 \alpha_1 x_1,$$

$$v_j = -\epsilon_j \alpha_j x_{j-1} x_j, \quad 1 < j < n,$$

$$v_n = -\epsilon_n \alpha_n x_n. \qquad (29)$$

Therefore, the solution of Eqs. (27) is obtained by inverting the band matrix P and reads

$$S_{a^j}(\infty) = \sum_{k=1}^{n} [P^{-1}]_{j,k} v_k. \qquad (30)$$

Having solved (at least formally) the set of equations (27) giving the stationary magnetization at each site a^j, the general one-dimensional stationary magnetization in the presence of n zealots simply reads.
(i) If $r < a^1$,

$$S_r(\infty) = S_{a^1}(\infty). \qquad (31)$$

(ii) If $a^j \leq r \leq a^{j+1}$ $(1 \leq j < n)$,

$$S_r(\infty) = S_{a^j}(\infty) + \frac{S_{a^{j+1}}(\infty) - S_{a^j}(\infty)}{a^{j+1} - a^j}(r - a^j). \qquad (32)$$

(iii) If $r > a^n$,

$$S_r(\infty) = S_{a^n}(\infty). \qquad (33)$$

As an example, let us consider the case where there are four zealots on the chain, as illustrated in Fig. 4. This figure shows that the one-dimensional stationary magnetization profile is a piecewise function, as predicted by Eqs. (31)–(33). When $n=4$, as in Fig. 4, Eqs. (27) explicitly read

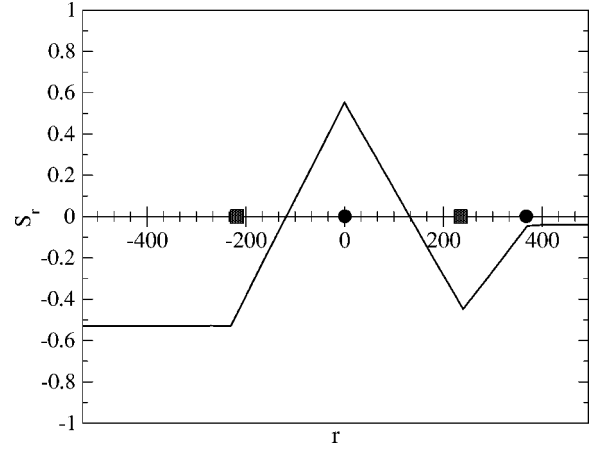$$S_{a^2}(\infty) - (1 + \alpha_1 x_1)S_{a^1}(\infty) = -\epsilon_1 \alpha_1 x_1,$$

FIG. 4. An example for numerical simulation of the case with four zealots on a $L = 1024$ lattice (see the text). The bias of the zealots from left to right is 0.01 (negative), 0.02 (positive), 0.013 (negative), and 0.003 (positive).

$$x_1 S_{a^3}(\infty) - (x_1 + x_2 + \alpha_2 x_1 x_2)S_{a^2}(\infty) + x_2 S_{a^1}(\infty) = -\epsilon_2 \alpha_2 x_1 x_2,$$

$$x_2 S_{a^4}(\infty) - (x_2 + x_3 + \alpha_3 x_2 x_3)S_{a^3}(\infty) + x_3 S_{a^2}(\infty) = -\epsilon_3 \alpha_3 x_2 x_3,$$

$$S_{a^3}(\infty) - (1 + \alpha_4 x_3)S_{a^4}(\infty) = -\epsilon_4 \alpha_4 x_3. \qquad (34)$$

The set of equations (34) can be solved explicitly and gives rise to very cumbersome expressions. Plugging into the latter the values corresponding to the system simulated in Fig. 4—i.e., $\alpha_1 = 0.01$, $\epsilon_1 = -1$, $\alpha_2 = 0.02$, $\epsilon_2 = +1$, $\alpha_3 = 0.013$, $\epsilon_3 = -1$, and $\alpha_4 = 0.003$, $\epsilon_4 = +1$, and $x_1 = 230$, $x_2 = 240$, and $x_3 = 130$—we obtain $S_{a^1}(\infty) = -0.529$, $S_{a^2}(\infty) = +0.556$, $S_{a^3}(\infty) = -0.441$, and $S_{a^4}(\infty) = -0.0367$. These values can be compared to the results of the simulations, reported in Fig. 4, where we obtained $S_{a^1}(\infty) = -0.53 \pm 0.01$, $S_{a^2}(\infty) = +0.55 \pm 0.01$, $S_{a^3}(\infty) = -0.45 \pm 0.01$, and $S_{a^4}(\infty) = -0.04 \pm 0.005$. These comparisons show that there is excellent agreement between the theoretical values predicted by the solution (30) of the system (34) and the numerical results. This agreement is somewhat surprising as the simulations reported in Fig. 4 have been carried on a relatively small system ($L = 1024$), whereas all the theoretical results (27)–(34) have been derived in the thermodynamic limit. This fact indicates that our analytic results may be quantitatively accurate even for large, but noninfinite, systems. In the limit where the strength of the zealots is $\alpha_1 = \ldots = \alpha_n = \infty$, all the expressions simplify and it follows from Eqs. (27) that $S_{a^j}(\infty) = \epsilon_j$, while, for $a^j \leq r \leq a^{j+1}$,

$$S_r(\infty) = \epsilon_j + \left(\frac{\epsilon_{j+1} - \epsilon_j}{a^{j+1} - a^j}\right)(r - a_j).$$

When $\alpha_1 = \ldots = \alpha_n = \infty$, this 1D system can be related to the one-dimensional spin model with Glauber dynamics (at zero temperature) in the presence of quenched random fields of infinite strength [18]: in the voter language, the situation considered by the authors of Ref. [18] would correspond to the case where at each site j a "voter" would have a probability p to be a zealot favoring the opinion $\epsilon_j = \pm 1$ with

strength $\alpha_j = \infty$ and would have a probability $1-2p$ to be an ordinary agent. The (slight) difference between such a model and the one studied in Ref. [18] is the fact that each zealot (even when he is endowed with an infinite strength) can be "forced" to flip by his two neighbors, while in Ref. [18] the (random) magnetic fields pin the spins along their direction. However, as $\alpha_j = \infty$, each zealot j rapidly flips back to his preferable opinion ϵ_j and thus both models are very close and display the same stationary magnetization.

We also would like to emphasize that the results (27) and (30) provide the exact magnetization of the completely disordered one-dimensional voter-model, where each site is endowed with a specific spin-flip rate. In this case, one would have $n = L \to \infty$ zealots in the system with $x_j = a^{j+1} - a^j = 1$, and the structure of the matrix P is rather simple [see Eq. (28)].

B. Results in 2D

In two dimensions, the integral of Eq. (4) is also divergent in the long-time regime $s \to 0$ and therefore its main contribution arises from $q^2 \equiv q_1^2 + q_2^2 \to 0$. In this sense, we first expand Eq. (4) for small s in the case when $\boldsymbol{r} = 0$:

$$\hat{I}_0(s) \xrightarrow[s \to 0]{} -\frac{1}{4\pi}\ln s. \tag{35}$$

More generally, for $r \gg 1$, we have (see Ref. [4])

$$\hat{I}_{\boldsymbol{r}}(s) \xrightarrow[s \to 0]{} \frac{1}{2\pi}K_0(r\sqrt{s}),$$

where $K_0(x)$ is the usual modified Bessel function of the third kind [20,21]. Using the small argument expansion of such a Bessel function we find that the long-time behavior for $t \gg r^2 \gg 1$ is given by

$$\hat{I}_{\boldsymbol{r}}(s) \xrightarrow[r\sqrt{s} \to 0]{} -\frac{1}{4\pi}[\ln(r^2 s) + 2\{\gamma - \ln 2\}], \tag{36}$$

where $\gamma = 0.5772156649\ldots$ denotes the usual Euler-Mascheroni's constant. From expression (20), when x is sufficiently large to use Eq. (36), we obtain the stationary magnetization of the zealots:

$$S_0(\infty) \simeq \frac{\alpha - \beta + \dfrac{\alpha\beta}{\pi}\ln x}{\alpha + \beta + \dfrac{\alpha\beta}{\pi}\ln x}$$

and

$$S_{\boldsymbol{x}}(\infty) \simeq \frac{\alpha - \beta - \dfrac{\alpha\beta}{\pi}\ln x}{\alpha + \beta + \dfrac{\alpha\beta}{\pi}\ln x}.$$

Interestingly these expressions resemble the ones obtained in 1D [see Eqs (23) and (24)]. The only change is in the dependence on separating distance: With respect to the 1D case, one has $x \to (1/\pi)\ln x$. When $r \gg 1$ and $|\boldsymbol{r} - \boldsymbol{x}| \gg 1$, from Eq. (20), using Eqs. (35) and (36), the stationary magnetization reads (see Fig. 5)
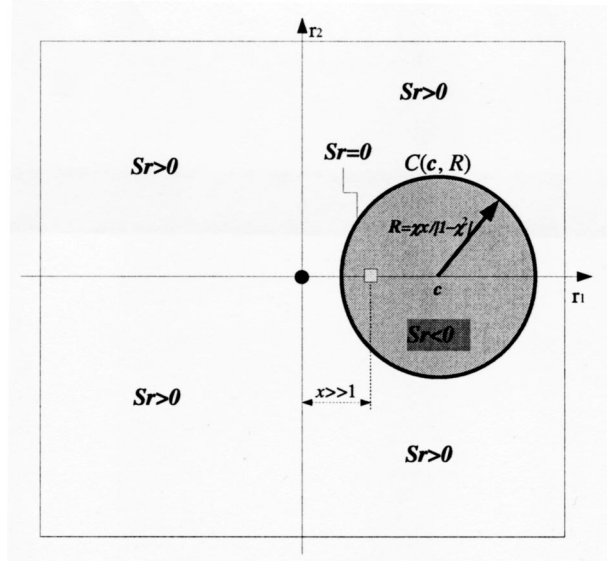

FIG. 5. Sketch of the typical 2D spatial dependence of the stationary magnetization when $L \to \infty$. At the origin, indicated by a dot, is the zealot favoring the state $+1$ with a strength $\alpha = 1$. At a distance $x \gg 1$, indicated by a square, is the zealot favoring the state -1 with a strength $\beta \simeq 0.9$. According to Eq. (37), the agents within the disk of center $c \simeq 2\boldsymbol{x}$ and of radius $R \simeq 1.4x$ have a negative final magnetization (denoted simply S_r in the figure). Outside the disk, the final magnetization of the agents is positive (see the text), while on the circle the agents are in a "neutral" final state. The static magnetization $S_r(\infty)$ exhibits both radial and polar dependence.

$$S_{\boldsymbol{r}}(\infty) \xrightarrow[r \gg 1, |\boldsymbol{r}-\boldsymbol{x}| \gg 1]{} \frac{\alpha - \beta - \dfrac{\alpha\beta}{\pi}\ln\dfrac{r}{|\boldsymbol{r}-\boldsymbol{x}|}}{\alpha + \beta + \dfrac{\alpha\beta}{\pi}[\ln x + \pi(\gamma - \ln 2)]}. \tag{37}$$

Far away from both zealots and in the case of sufficiently separated zealots—i.e., $r \gg x \gg 1$—this expression simplifies:

$$S_{\boldsymbol{r}}(\infty) \xrightarrow[r \gg x \gg 1]{} \frac{\alpha - \beta - \dfrac{\alpha\beta}{\pi}\dfrac{x}{r}\cos\theta}{\alpha + \beta + \dfrac{\alpha\beta}{\pi}[\ln x + \pi(\gamma - \ln 2)]}, \tag{38}$$

where $\cos\theta \equiv (\boldsymbol{r} \cdot \boldsymbol{x})/rx$. Here we used the fact that $\ln(r/|\boldsymbol{r} - \boldsymbol{x}|) = x\cos\theta/r + O((x/r)^2)$, when $r \gg x \gg 1$. These results show that, because of the competition between the two zealots, the stationary magnetization is a fluctuating steady state exhibiting nontrivial radial and polar dependence. Also, when $\alpha = \beta = \infty$, Eq. (37) reduces to

$$S_{\boldsymbol{r}}(\infty) \xrightarrow[r \gg 1, |\boldsymbol{r}-\boldsymbol{x}| \gg 1]{} \frac{\ln\dfrac{|\boldsymbol{r}-\boldsymbol{x}|}{r}}{\ln x + \pi(\gamma - \ln 2)}$$

and $S_0(\infty) = -S_{\boldsymbol{x}}(\infty) = 1$.

Regarding the dynamical behavior, in the regime where $t \gg \max(|\boldsymbol{r} - \boldsymbol{x}|^2, r^2)$, the long-time behavior of the magnetization is the following:

$$S_{\boldsymbol{r}}(t) - S_{\boldsymbol{r}}(\infty) \simeq -\frac{1}{\ln t} \left[\frac{\ln \frac{r^{2\alpha}}{|\boldsymbol{r}-\boldsymbol{x}|^{2\beta}} - \frac{\alpha\beta}{\pi} \ln \frac{r}{|\boldsymbol{r}-\boldsymbol{x}|} \{\ln(x/2) + \gamma\} + 2(\alpha-\beta)(\gamma-\ln 2)}{\alpha + \beta + \frac{\alpha\beta}{\pi}\{\ln x + \pi(\gamma - \ln 2)\}} \right]. \tag{39}$$

In the situation where $r \gg x \gg 1$, the above expression simplifies and the approach toward the steady state, Eq. (38), is

$$S_{\boldsymbol{r}}(t) - S_{\boldsymbol{r}}(\infty) \simeq -\frac{1}{\ln t} \left[\frac{2\left[(\alpha-\beta)\ln r + \frac{x}{r}\beta\cos\theta \right] - \frac{\alpha\beta}{\pi}\left\{ \frac{x}{r}\cos\theta\ln x \right\}}{\alpha + \beta + \frac{\alpha\beta}{\pi}\{\ln x + \pi(\gamma - \ln 2)\}} \right].$$

For $t \gg r^2$, these results tell us that the 2D system evolves logarithmically slowly toward a space-dependent fluctuating steady state. As in the presence of only one zealot, we can see that in 2D the magnetization does not exhibit a scaling expression between r and t when $r^2 \sim t \gg 1$ [4]. This is due to the logarithmic terms, specific to the two-dimensional situation, appearing in Eqs. (35) and (36). Natural questions arise regarding the spatial distribution of "opinions:" *What is the spatial voting distribution in the steady state? Which region is characterized by a majority of positive and negative opinion? How does the strength of α and β affect the final spatial opinion distribution?*

To answer these questions, we use Eq. (37) and notice that in the limit $r \gg 1$ and $|\boldsymbol{r}-\boldsymbol{x}| \gg 1$, the spatial region where $S_{\boldsymbol{r}}(\infty) = 0$ obeys the equation

$$\frac{r}{|\boldsymbol{r}-\boldsymbol{x}|} = \chi^{-1} \text{ with } \chi \equiv \exp\left(\frac{\pi[\beta-\alpha]}{\alpha\beta} \right). \tag{40}$$

When $\alpha \neq \beta$—i.e., for $\chi \neq 1$—such an equation can be recast into the following form

$$r^2 + \frac{2rx}{\chi^2 - 1}\cos\theta - \frac{x^2}{\chi^2 - 1} = 0,$$

i.e., the polar equation of a circle $\mathcal{C}(\boldsymbol{c}, R)$ centered at $\boldsymbol{c} = [1/(1-\chi^2)]\boldsymbol{x}$ and of radius $R = \chi x/|1-\chi^2| = x/2\sinh(|\alpha^{-1} - \beta^{-1}|)$. This result, together with Eqs. (37) and (40), implies that in 2D, for $\alpha \neq \beta$, the agents located on the circle $\mathcal{C}(\boldsymbol{c}, R)$ are "neutral" and they have zero final magnetization as illustrated in Fig. 5. From Eqs. (37) and (40) we can also conclude the following.

(i) If $\chi > 1$—i.e., $\beta > \alpha$—the agents that are within (outside) the disk Int $\mathcal{C}(\boldsymbol{c}, R)$ have a positive (negative) magnetization.

(ii) If $\chi < 1$—i.e., $\beta < \alpha$—the agents that are within (outside) the disk Int $\mathcal{C}(\boldsymbol{c}, R)$ have a negative (positive) magnetization. This case is sketched in Fig. 5.

These results show that the majority of the voters, except the ones enclosed in the disk, tend to follow the opinion favored by the strongest zealot. The details of the neutral region $\mathcal{C}(\boldsymbol{c}, R)$ depends nontrivially on all the parameters α, β, and $\boldsymbol{x}$ and, interestingly, the radius grows with the difference of the strength of the zealots as $R \propto 1/\sinh u$, where

$u \equiv \beta^{-1} - \alpha^{-1}$. Also, R increases linearly with the separating distance x.

(iii) The case $\alpha = \beta$ (including $\alpha = \beta = \infty$)—i.e., $\chi = 1$—is special. In this situation, it follows from Eq. (40) that the region with zero final magnetization is no longer a closed curve but an infinite line given by the equation $r = x/2\cos\theta$ which separates the two-dimensional space into two semi-infinite half-planes.

For the number of zealots $n > 2$ the analytical calculations become very tedious and we illustrate the results of a Monte Carlo simulation of the case with six zealots in Fig. 6. The simulation is carried on a (128×128) lattice, and due to the $1/\ln(t)$ approach to the steady state, enormous sampling times are required. Again when simulating the system one has to be careful with the sites on the boundaries: if the site lies on the edges, then it has only three nearest neighbors, and if it is at the corners, then it has only two nearest neighbors. The stochastic rules have to be slightly modified to account for the boundary sites. The geometry of the zealots can be seen from contour plot in Fig. 6 where three of the zealots are positively biased and three are biased negatively. The left picture in Fig. 6 shows the average magnetization $S_{\boldsymbol{r}}(\infty)$ on the different sites of the lattice. For these particular values of the bias of the zealots and their position on the lattice, in the stationary state, we observe one large region of positive on average opinion (a curved central "stripe" in Fig. 6) and two smaller disconnected regions of a negative opinion (near the left boundary and top right edge of Fig. 6).

Regarding the coarsening of the 2D system, we again distinguish three situations: (i) when $n < 2$, there is usual coarsening and an infinite domain eventually spans the entire system; (ii) when there is a finite number of competing zealots, large domains still develop but their size is limited by the zealots; (iii) when the density of the competing zealots is finite in the thermodynamic limit, there is no longer coarsening as the formation of large domains is prevented by the interaction with the numerous inhomogeneities.

To conclude this section, as in 1D, we notice that $\alpha[1 - S_{\boldsymbol{0}}(\infty)] = \beta[1 + S_{\boldsymbol{x}}(\infty)]$ which implies, with Eq. (18), that the global magnetization evolves, following the strongest zealot ($\alpha \neq \beta$), as $M(t) \sim t/\ln t$. As a consequence, the time T necessary for the strongest zealot to dominate (on average) the whole 2D system is $T \sim L^2 \ln L$ (where $L \to \infty$). In the
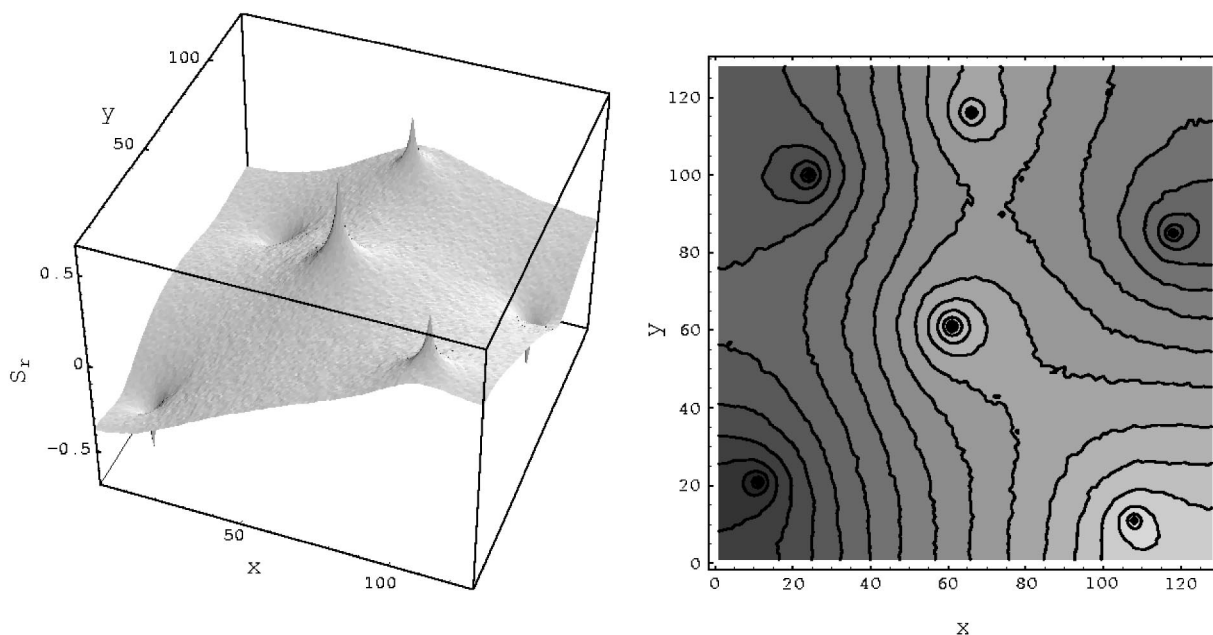
FIG. 6. The stationary site magnetization $S_r(\infty)$ on a (128×128) lattice in the presence of six zealots. Three of the zealots favor the $+1$ state and other three the -1 opinion. The picture on the left shows a 3D plot of $S_r(\infty)$ (along the vertical axis) and the picture on the right is the corresponding contour plot. The strengths of the positive zealots are 2.0, 1.2, 0.8 and the strengths of the negative ones are 1.6, 1.4, 1.0.

symmetric case $(\alpha = \beta)$, as explained above, the 2D space is exactly separated in two semi-infinite half-planes with opposite total magnetization.

C. Results in 3D

Above two dimensions, the integrals in Eq. (4) are well defined for all values of s and in particular when $s \to 0$. Therefore, in contrast to what happens in 1D and 2D, to determine the long-time behavior of the magnetization we cannot simply focus on the $q \to 0$ expansion of Eq. (4). This also means that in dimensions $d \geqslant 3$ in the presence of n zealots the static magnetization readily follows from Eq. (16):

$$S_r(\infty) = \sum_{j=1}^{n} \sum_{\ell=1}^{n} \epsilon_\ell \hat{I}_{a^j - r}(0) [\mathcal{N}^{-1}(0, \{\alpha\})]_{j,\ell}. \tag{41}$$

The three-dimensional lattice Green function $\hat{I}_r(0)$ has been computed very recently by Glasser and Boersma [22]. Using the triplet (a_r, b_r, c_r) of rational numbers depending on r, given in Table 2 of Ref. [22], and the quantity $g_0 \equiv ((\sqrt{3} - 1)/96\pi^3)\Gamma^2(1/24)\Gamma^2(11/24) = 0.505462\ldots$ [$\Gamma(z)$ is Euler's gamma function], it has been established that

$$\hat{I}_r(0) = \frac{1}{2}\left[a_r g_0 + c_r + \frac{b_r}{\pi^2 g_0}\right]. \tag{42}$$

With Eqs. (20) and (42) the exact expression of the three-dimensional magnetization in the presence of two zealots is explicitly given by

$$S_r(\infty) = \frac{\alpha\epsilon_1\hat{I}_r(0) + \beta\epsilon_2\hat{I}_{r-x}(0) + \alpha\beta\{\hat{I}_r(0)[\epsilon_1\hat{I}_0(0) - \epsilon_2\hat{I}_x(0)] + \hat{I}_{r-x}(0)[\epsilon_2\hat{I}_0(0) - \epsilon_1\hat{I}_x(0)]\}}{1 + (\alpha + \beta)\hat{I}_0(0) + \alpha\beta[\hat{I}_0^2(0) - \hat{I}_x^2(0)]}. \tag{43}$$

From now on, for the sake of concreteness, we focus on the case where we have two competing zealots, $\epsilon_1 = -\epsilon_2 = 1$, and thus expression (43) becomes

$$S_r(\infty) = \frac{\alpha\hat{I}_r(0) - \beta\hat{I}_{r-x}(0) + \alpha\beta[\hat{I}_r(0) - \hat{I}_{r-x}(0)][\hat{I}_0(0) + \hat{I}_x(0)]}{1 + (\alpha + \beta)\hat{I}_0(0) + \alpha\beta[\hat{I}_0^2(0) - \hat{I}_x^2(0)]}.$$

As we are mainly interested in the large-r limit, one can observe that $\hat{I}_r(0)$ is just the static solution of the Poisson equation $\Delta_r \hat{I}_r(0) = -\delta_{r,0}$, which solution in the continuum limit is $\hat{I}_r(0) \simeq \hat{\mathcal{I}}(r) = 1/4\pi r$ $(r > 0)$. This result, obtained from an "electrostatic reformulation," is valid on the discrete lattice for $r \gg 1$.[1] With the help of Eq. (43), this result allows us to compute the 3D stationary local magnetization for $r \gg 1$ and $|r - x| \gg 1$:

$$S_r(\infty) = -\frac{1}{4\pi}\left[\frac{\mathcal{C}_1}{r} + \frac{\mathcal{C}_2}{|r - x|}\right], \qquad (44)$$

where $\mathcal{C}_1 = -2\alpha/(2 + \alpha g_0)$ and $\mathcal{C}_2 = 2\beta/(2 + \beta g_0)$. Again, the resemblance with electrostatics is striking: the static magnetization is formally the electrostatic potential generated by the "charges" $\mathcal{C}_1$ at site 0 and $\mathcal{C}_2$ at x. As already noticed, the difficulty resides in the fact that the charges $\mathcal{C}_1$ and $\mathcal{C}_2$ are *a priori* unknown and have been computed in a *self-consistent* way (assuming a large enough separating distance x), with the help of the exact and discrete results (42) and (43).[2] Even though the result (44) is formally valid for $r \gg x \gg 1$, as explained above, it gives already accurate predictions when $r \gg 1$ and x is finite but large enough (e.g., already when $x \geq 6$). It is suggestive that in the limit where $\alpha = \beta = \infty$, the "charges" $\mathcal{C}_2 = -\mathcal{C}_1 = 2/g_0$. In this case the magnetization in Eq. (44) can be viewed as the potential of the electric dipole of charges $\pm 2/g_0$. To make the connection with electrostatics even more transparent, it is worthwhile to notice that the expression (44) can be rewritten using a *multipole expansion*. Also, when $\beta = 0$, we recover $S_r(\infty) \propto 1/r$, as reported in Ref. [4]. In fact, one has $|r - x|^{-1} = (r^2 + x^2 - 2r \cdot x)^{-1/2} = (1/r)\sum_{m=0}^{\infty}(x/r)^m P_m(\cos\theta)$, where $\cos\theta \equiv (x \cdot r)/xr$ and the $P_m(\cos\theta)$ are the Legendre polynomials. Thus expression (44) can be recast into

$$S_r(\infty) = -\frac{1}{4\pi r}\left[\mathcal{C}_1 + \mathcal{C}_2 \sum_{m=0}^{\infty}\left(\frac{x}{r}\right)^m P_m(\cos\theta)\right]. \qquad (45)$$

At this point it is important to mention a major difference with the case where only a single zealot is present. In the latter situation, as showed in Ref. [4], just by taking the continuum limit of the equation for the magnetization, one could anticipate that $S_r(\infty) \propto r^{-1}$ (i.e., it has only radial dependence) in three dimensions, which is the main desired information. In the two-zealot case, as there is a competition between the effects of the "charges" $\mathcal{C}_1$ and $\mathcal{C}_2$, we really need to determine $S_r(\infty)$ through Eqs. (42) and (43), to obtain the nontrivial spatial dependence of the stationary magnetization through Eqs. (44) and (45).

Regarding the dynamical approach toward the steady state, it is difficult to study the small s behavior of $\hat{I}_r(s)$ and to rigorously obtain the long-time approach toward the stationary magnetization. However, it follows from Eq. (17) that

$$S_r(t) - S_r(\infty) \approx \frac{1}{2\pi(4\pi t)^{1/2}}[\mathcal{C}_1 e^{-r^2/4t} + \mathcal{C}_2 e^{-|r - x|^2/4t}].$$
$$(46)$$

This result is expected to be accurate in the regime where $t \to \infty$, $r \gg 1$, and $|r - x| \gg 1$. As previously mentioned, we can discuss about the regions with positive or negative stationary magnetization. To determine the "neutral" region [where $S_r(\infty) = 0$] it follows from Eq. (44) that, in the limit where $r \gg 1$ and $|r - x| \gg 1$, one has to solve

$$\frac{r}{|r - x|} = \delta^{-1} \text{ with } \delta \equiv \left|\frac{\mathcal{C}_2}{\mathcal{C}_1}\right| = \frac{\beta(2 + \alpha g_0)}{\alpha(2 + \beta g_0)}. \qquad (47)$$

When $\alpha \neq \beta$—i.e., for $\delta \neq 1$—the equation can again be recast into the following form:

$$r^2 + \frac{2rx}{\delta^2 - 1}\cos\theta - \frac{x^2}{\delta^2 - 1} = 0.$$

Such an expression is the polar equation of a sphere $\Sigma(C, \mathcal{R})$ centered at $C = [1/(1 - \delta^2)]x$ with a radius $\mathcal{R} = \delta x/|1 - \delta^2|$. From Eq. (44), we can also infer the following.

(i) If $\delta > 1$—i.e., $\beta > \alpha$—the agents that are within (outside) the sphere $\Sigma(c, R)$ have a positive (negative) magnetization.

(ii) If $\delta < 1$—i.e., $\beta < \alpha$—the agents that are within (outside) the sphere $\Sigma(C, \mathcal{R})$ have a negative (positive) magnetization.

These results show that majority of the voters, except the ones enclosed in the sphere $\Sigma(C, \mathcal{R})$, tends to follow the opinion favored by the strongest zealot. The details of the neutral region $\Sigma(C, \mathcal{R})$ depend nontrivially on all the parameters α, β, and x. In particular, we notice that $\mathcal{R}$ increases linearly with the separating distance x.

(iii) The case where $\alpha = \beta$—i.e., $\delta = 1$—is special because thus the "effective charges" are such that $|\mathcal{C}_1| = \mathcal{C}_2$. In particular, this is the case when $\alpha = \beta = \infty$. It thus follows from Eq. (47) that the region with zero final magnetization is no longer a surface but an infinite plane, given by $r = x/2\cos\theta$, that separates the 3D space into two regions.

In 3D, $\alpha[1 - S_0(\infty)] \neq \beta[1 + S_x(\infty)]$ when $\alpha \neq \beta$, and thus the global magnetization of the above inhomogeneous voter model evolves linearly with the time: $M(t) \sim t$. This implies that the time T necessary for the strongest zealot to dominate (on average) the whole 3D system scales as $T \sim L^3$, where $L \to \infty$. On the other hand, when $\alpha = \beta$, the space is divided in two symmetric regions with opposite total magnetization.

---

[1] We have compared the continuum result to the exact expression (42) and have noticed that the discrete and continuum expressions are very close, even for finite values of r: for instance, at site $r = (5, 3, 1)$, we have exactly $\hat{I}_r(0) = 0.01344\ldots$, whereas the "electrostatic" reformulation gives $\hat{\mathcal{I}}(r) = 1/4\pi\sqrt{35} = 0.01345\ldots$. This shows that, already for r finite, the latter reformulation is an excellent approximation of Eq. (42).

[2] In three dimensions, in the presence of n zealots at sites $\{a^1, \ldots, a^n\}$, using a continuum electrostatic reformulation (which is valid if $|r - a^1| \gg 1, \ldots, |r - a^n| \gg 1$), we can infer in the same manner: $S_r(\infty) = -(1/4\pi)[C_1/|r - a^1| + \cdots + C_n/|r - a^n|]$, which can be developed in multipolar expansion. In general, to compute the "charges" $C_1, \ldots, C_n$ one needs to explicitly invert the matrix $\mathcal{N}$.

Finally, in the case where both zealots favor the same opinion $\epsilon = \pm 1$—i.e., $\epsilon_1 = \epsilon_2 = \epsilon$—one has just to modify the expressions of "charges" in Eqs. (44)–(46). In fact, these results are still valid with $\mathcal{C}_1 = -2\epsilon\alpha/(2 + \alpha g_0)$ and $\mathcal{C}_2 = -2\epsilon\beta/(2 + \beta g_0)$.

V. MONOMER-MONOMER CATALYTIC REACTION ON AN INHOMOGENEOUS SUBSTRATE

The other model that we specifically consider in this work is the monomer-monomer catalytic reaction. Such a process is of considerable interest in many fields of science and the technology. In the catalysis the rate of a chemical reaction is enhanced by the presence of a suitable catalytic material, such as the platinum used to catalyze the oxidation of carbon monoxide $(2\mathrm{CO} + \mathrm{O}_2 \rightarrow 2\mathrm{CO}_2)$ [19,23]. Because of the numerous and practical implications of the catalytic reaction, it is of prime interest to be able to model its quantitative and qualitative behavior. In general, these processes are described within mean-field like approaches where it is assumed that molecules are randomly distributed on the substrate [19,23]. Spatial fluctuations and excluded volume constraints are thus ignored, despite of the fact that these effects are shown to play often a crucial role [24].

In the modeling of catalysis [23], the monomer-monomer surface reaction model plays an important part at least from a theoretical point of view because the simplicity of the model allows to address several issues analytically, such as the role of the fluctuations [5,24], the interfacial roughening [25], and the diffusion of the adsorbents [26].

The monomer-monomer catalytic process on a homogeneous substrate is by now well understood and it comprises the following reactions [5,6]:

$$A + \varnothing \xrightarrow{k_A} A_S,$$

$$B + \varnothing \xrightarrow{k_B} B_S,$$

$$A_S + B_S \xrightarrow{k_r} AB\uparrow + 2\varnothing.$$
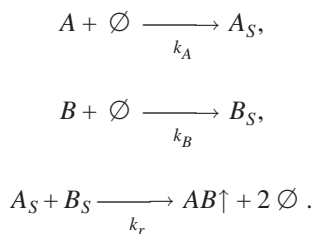
The A and B particles impinge upon a substrate with rates k_A and k_B, respectively, adsorb onto vacant sites $(\varnothing)$ and form monolayers of adsorbed particles, A_S and B_S. Nearest-neighbor pairs of different adsorbed particles, $A_S B_S$, react and desorb with rate k_r, leaving two vacant sites $(2\varnothing)$ on the substrate. The dynamics on a spatially homogeneous substrate is most interesting in dimensions $d \le 2$, when $k_A = k_B$ (otherwise the species with the bigger rate will rapidly saturate the substrate). In this case there is coarsening on the substrate induced by fluctuations and islands of A_S and B_S particles grow. As in Refs. [5,6], we will consider the reaction-controlled limit, where $k_r \ll k_A = k_B$. This limit turns out to be useful from a technical point of view and, most importantly, provides qualitatively the same kind of behavior as the general case [5,6,24]. In the reaction-controlled limit, the substrate quickly becomes fully occupied and stays covered with A_S's and B_S's for ever (vacancies are immediately refilled). The kinetics of monomer-monomer substrate reaction model is therefore a *two-state* system that can be mapped onto the voter model supplemented by an infinite-temperature Kawasaki exchange process [5,6]. In fact, in the monomer-monomer catalytic reaction under consideration, A_S and B_S desorb and the resulting empty sites are instantaneously refilled either by $A_S B_S$ (no reaction), $A_S A_S, B_S B_S$ (voter dynamics), or $B_S A_S$ (Kawasaki exchange dynamics at infinite temperature).

Clearly, more realistic situations should include the presence of inhomogeneities which could deeply affect the properties of the system. In fact, real substrates (in 1D and 2D) display generally some degrees of spatial heterogeneity which are attributed to imperfections, such as dislocations and defects [27] that modify locally the interactions on the substrate. In some previous works translationally invariant disordered models catalysis have been considered within mean-field-like approaches—i.e., rate equations and pair approximation [28]. In these works, it was shown that quenched substrate imperfections dramatically affect the dynamics, resulting in a reactive steady state. One should emphasize that both the physical systems (in this work, the inhomogeneities are not randomly distributed but fixed) and analytic methods (we obtain exact results in arbitrary dimensions, while the authors of [28] employed mean-field-like approaches) considered here differ from, and are thus complementary to, those of Ref. [28]. Also, very recently, an *equilibrium* model for monomer-monomer catalysis on a disordered substrate was solved [29].
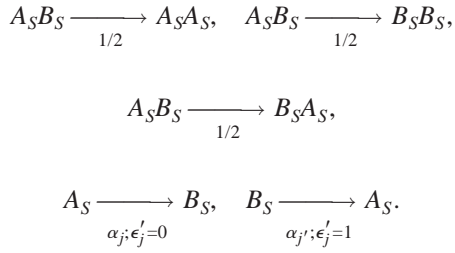
Hereafter we study the static and dynamical effects of local inhomogeneities in the monomer-monomer catalytic reaction-controlled process and show how to take advantage of the results obtained for the inhomogeneous voter model to infer some exact properties. In fact, we consider the *genuine nonequilibrium* situation where the substrate is *spatially inhomogeneous*, because of the presence of a collection of n inhomogeneities located at sites $\{a^j\}, j = 1, \dots, n$, favoring the local adsorption of A's or B's. We show that the inhomogeneities induce spatially dependent reactive steady state when $n > 1$. As a substrate, as described in Sec. II, we consider a hypercubic lattice with $(2L+1)^d$ sites and introduce a set of parameters $\epsilon'_{j'}$, taking the values 0 or 1, and consider, in addition to the usual homogeneous catalytic reaction described above, that some inhomogeneities *locally* favor the presence of A via desorption of B's (and vice versa) through the additional reactions

$$B_S \xrightarrow{\alpha_j} A_S,$$

where $\epsilon'_j = 1$, and

$$A_S \xrightarrow{\alpha_{j'}} B_S,$$
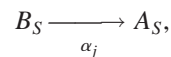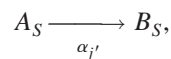
where $\epsilon'_{j'} = 0$. We therefore consider the following homogeneous processes (voter+infinite-temperature Kawasaki dynamics), all occurring with the same rates $1/2$, and local (inhomogeneous) reactions at sites a^j and $a^{j' \ne j}$, occurring, respectively, with rates α_j and $\alpha_{j'}$:

$$A_SB_S \xrightarrow[1/2]{} A_SA_S, \quad A_SB_S \xrightarrow[1/2]{} B_SB_S,$$

$$A_SB_S \xrightarrow[1/2]{} B_SA_S,$$

$$A_S \xrightarrow[\alpha_j; \epsilon'_j=0]{} B_S, \quad B_S \xrightarrow[\alpha_{j'}; \epsilon'_j=1]{} A_S.$$

Here, the bimolecular reactions correspond to the voter dynamics supplemented by Kawasaki infinite-temperature exchange process, whereas monomolecular processes correspond to reactions induced by local inhomogeneities favoring the adsorption of one species. Following the same steps as in Refs. [5,6], for this spatially inhomogeneous monomer-monomer catalytic process, in the thermodynamic limit we obtain the following equation of motion for the concentration $c_r(t)$ of A_S at site r of the substrate:

$$\frac{d}{dt}c_r(t) = \Delta_r c_r(t) + \sum_{j=1}^{n} \alpha_j[\epsilon'_j - c_{a^j}(t)]\delta_{r,a^j}. \quad (48)$$

Of course, the concentration of B_S at site r is simply given by $1-c_r(t)$. The resemblance of Eq. (48) with Eq. (3) is striking (the only difference is that here $\epsilon'_j=0,1$) and one can immediately infer the solution of Eq. (48) from Eqs. (15) and (20). In particular, in the thermodynamic limit, starting from a system initially completely occupied by B_S particles, the Laplace transform of the concentration of A_s reads

$$\hat{c}_r(s) = \frac{1}{s}\sum_{j,\ell} \epsilon'_\ell \hat{I}_{a^j-r}(s)[\mathcal{N}^{-1}(s,\{\alpha\})]_{j,\ell}, \quad (49)$$

and we get, for the time-dependent concentration [initially $c_r(0)=0$],

$$c_r(t) = \frac{1}{2\pi i}\int_{c-i\infty}^{c+i\infty} \frac{ds}{s} e^{st}\sum_{j,\ell} \epsilon'_\ell \hat{I}_{a^j-r}(s)[\mathcal{N}^{-1}]_{j,\ell}. \quad (50)$$

In this language, the quantity

$$M'(t) \equiv \sum_{k} c_k(t) = \sum_{j=1}^{n} \alpha_j \int_0^t d\tau[\epsilon'_j - c_{a^j}(\tau)] \quad (51)$$

provides the average total number of the A_S particles on the substrate at time t.

Next, we restrain ourself to physical situations and consider in detail the monomer-monomer catalytic reaction in the presence of one and two inhomogeneities in one and two dimensions.

A. Inhomogeneous monomer-monomer catalytic reaction in the presence of one single "defect"

Here, we consider the case where there is a single inhomogeneity at site $a^1=0$, with strength $\alpha_1=\alpha$ and $\epsilon_1=1$. In this case, we simply have $\mathcal{N}^{-1}=\alpha/[1+\alpha\hat{I}_0(s)]$. Therefore, starting from a system initially full of B_S particle [i.e., $c_r(0)=0$] we obtain

$$\hat{c}_r(s) = \frac{1}{s}\frac{\alpha\hat{I}_r}{1+\alpha\hat{I}_0(s)}. \quad (52)$$

On the right-hand side of this equation, one recognizes immediately the same expression as the Laplace transform of the magnetization obtained in Ref. [4]. From previous results, we can immediately infer the long-time behavior of the concentration of A_s particles.

1. Results in 1D

Following the same steps as in Ref. [4], on a one-dimensional substrate we find from Eq. (52) that the long-time behavior of the concentration of A_S reads

$$c_r(t) \simeq 1 - \frac{r+2/\alpha}{\sqrt{\pi t}}. \quad (53)$$

This result is valid for any $0 \leq r < \infty$.

When both $r \to \infty$ and $t \to \infty$, we obtain the following simple scaling expression [4]:

$$c_r(t) \simeq \text{erfc}\left(\frac{r}{2\sqrt{t}}\right). \quad (54)$$

2. Results in 2D

In two dimensions, following results from Ref. [4] we obtain a nonscaling expression for the concentration, with very slow time dependence:

$$c_0(t) - c_0(\infty) \simeq -\left(\frac{4\pi}{\alpha}\right)\frac{1}{\ln t}, \quad (55)$$

where $c_0(\infty)=1$. For the other sites, we find that the long-time behavior in the regime $t \gg r^2 \gg 1$ is given by

$$c_r(t) - c_r(\infty) \simeq -\frac{\ln r^2}{\ln t}, \quad c_r(\infty)=1. \quad (56)$$

As in the one-dimensional case, the stationary concentration of A_S corresponds again to a substrate fully covered with A_S particles—i.e., $c_r(\infty)=1$. Therefore, the presence of a single inhomogeneity favoring locally the adsorption of A_S is enough to completely cover the substrate with A_S in spite of the fact that initially only B_S particles were present. From expressions (53), (55), and (51), we can also compute the total number of A_S particles on the substrate at time $t \gg 1$. In so doing, one obtains $M'(t) \sim \sqrt{t}$ in the one-dimensional case and $M'(t) \sim t/\ln t$ in 2D.

B. Inhomogeneous monomer-monomer catalytic reaction in the presence of two defects

Here, we consider the case where two "competing" inhomogeneities are present: one is at site $a^1=0$, with strength $\alpha_1=\alpha$ and $\epsilon_1=1$ and the other at site $a^2=x$, with strength $\alpha_2=\beta$ and $\epsilon_2=0$.

In this case, using Eqs. (49) and (11), we obtain the following expression for the Laplace transform of the concentration of A_s at site r, starting from $c_r(0)=0$:

$$\hat{c}_r(s) = \frac{1}{s} \sum_{j,\ell} \hat{I}_{a^j-r}(s) \epsilon'_\ell [\mathcal{N}^{-1}(s,\{\alpha\})]_{j,\ell}$$

$$= \frac{\alpha \hat{I}_r(s) + \alpha\beta[\hat{I}_r(s)\hat{I}_0(s) - \hat{I}_{r-x}(s)\hat{I}_x(s)]}{s\{1 + (\alpha+\beta)\hat{I}_0(s) + \alpha\beta[\hat{I}_0^2(s) - \hat{I}_x^2(s)]\}}. \quad (57)$$

1. Results in 1D

In one dimension, without loss of generality, we assume that the inhomogeneity at site $a^2 = x$, $x = |x|$ is on the right side of the origin.

Proceeding as in Sec. IV A, we study the static and long-time behavior of the concentration of A_S with $c_r(0) = 0$, and distinguish various situations.

(i) For sites between the two inhomogeneities—i.e., $0 \leq r \leq x$—we get

$$c_r(t) \simeq \frac{\alpha[1 + \beta(x-r)]}{\alpha+\beta+\alpha\beta x} - \left(\frac{\alpha}{\alpha+\beta+\alpha\beta x}\right)$$
$$\times \frac{1}{\sqrt{\pi t}} \left\{ r + \frac{[1+\beta(x-r)](2 - \alpha\beta x^2/2)}{\alpha+\beta+\alpha\beta x} \right\}. \quad (58)$$

(ii) At the right of the origin, when $x < r < \infty$, we obtain

$$c_r(t) \simeq \frac{\alpha}{\alpha+\beta+\alpha\beta x} \left[1 - \frac{1}{\sqrt{\pi t}} \left\{ r + \frac{2 - \alpha\beta x^2/2}{\alpha+\beta+\alpha\beta x} \right\} \right]. \quad (59)$$

(iii) At the left of the origin, when $0 < r < \infty$, we find

$$c_{-r}(t) \simeq \frac{\alpha}{\alpha+\beta+\alpha\beta x} \left[1 + \beta x - \frac{1}{\sqrt{\pi t}} \right.$$
$$\left. \times \left\{ r + \frac{(1+\beta x)(2 - \alpha\beta x^2/2)}{\alpha+\beta+\alpha\beta x} \right\} \right]. \quad (60)$$

(iv) When both $t \to \infty$ and $r \to \infty$, we have

$$c_r(t) \simeq \frac{\alpha}{\alpha+\beta+\alpha\beta x} \, \text{erfc}\left(\frac{r}{2\sqrt{t}}\right), \quad (61)$$

$$c_{-r}(t) \simeq \frac{\alpha(1+\beta x)}{\alpha+\beta+\alpha\beta x} \, \text{erfc}\left(\frac{r}{2\sqrt{t}}\right). \quad (62)$$

These results show that in the interval between the inhomogeneities, the static concentration profiles varies linearly from the origin with a slope $-\alpha\beta/(\alpha+\beta+\alpha\beta x)$. Outside from this interval, the static concentration is uniform on the right and left side of the origin: on the right, $c_r(\infty) = \alpha(1 + \beta x)/(\alpha+\beta+\alpha\beta x)$, whereas on the left $c_r(\infty) = \alpha/(\alpha+\beta + \alpha\beta x)$. Such a static profile can again be interpreted as the solution of a discrete 1D electrostatic Poisson equation with peculiar and suitable boundary conditions. Again, the static concentration is reached according to a power law $[c_r(t) \sim t^{-1/2}]$ and with amplitudes depending nontrivially on all parameters of the system. At very large distances and long time, the concentration displays a scaling form which amplitude depends on which inhomogeneity is the closest. Of

course, it is easy to check that in the limit $\alpha \to 0$, as the system is initially full of B_S, then $c_r(t) = 0$. Also, when $\beta = 0$, we recover expressions (53) and (54). From Eqs. (51) and (58) we obtain the average number of adsorbed particles which evolves (at long time) as $M'(t) \sim \sqrt{t}$.

Again, in one dimension we can obtain the stationary concentration of adsorbed A_S particle in the completely disordered case—i.e., when n is arbitrary large—just by replacing, respectively, $S_{a^j}(\infty), S_r(\infty), \epsilon_j$ by $c_{a^j}(\infty), c_r(\infty), \epsilon'_j$ in expressions (27)–(33). As illustrated in Fig. 4, in this case the stationary concentration profile is piecewise. Also, when the number of competing inhomogeneities is finite the system coarsens as described in Sec. IV A.

2. Results in 2D

In two dimensions and at large distance from both inhomogeneities—i.e., for $r \gg 1$ and $|r - x| \gg 1$—we find a nonscaling expression for both static and time-dependent concentrations of the A_S particles,

$$c_r(\infty) \simeq \frac{\alpha - \frac{\alpha\beta}{2\pi}\left[\ln\left(\frac{r}{x|r-x|}\right) - \pi(\gamma - \ln 2)\right]}{\alpha+\beta+\frac{\alpha\beta}{\pi}[\ln x + \pi(\gamma - \ln 2)]}, \quad (63)$$

and, when x is large enough:

$$c_0(\infty) \simeq \frac{\alpha\left(1 + \frac{\beta}{\pi}\ln x\right)}{\alpha+\beta+\frac{\alpha\beta}{\pi}\ln x} \quad \text{and} \quad c_x(\infty) \simeq \frac{\alpha}{\alpha+\beta+\frac{\alpha\beta}{\pi}\ln x}.$$

We can notice that in 2D the stationary concentration of the A_S particles is a fluctuating reactive state exhibiting nontrivial radial and polar dependence. Regarding the approach toward the steady state, proceeding as in Sec. IV B, we obtain

$$c_r(t) - c_r(\infty) \simeq -\frac{B'(r,x)}{\ln t}, \quad (64)$$

where the amplitude

$$B' = \frac{\frac{\alpha\beta}{\pi}\ln x\{\ln|r-x| + \gamma - \ln 2\} + 2\alpha\ln r}{\alpha+\beta+\frac{\alpha\beta}{\pi}[\ln x + \pi(\gamma - \ln 2)]}$$

exhibits a nontrivial spatial dependence. Again, the result (64) shows that the stationary concentration profile (63) is reached logarithmically slowly. Using Eq. (51) we can also notice that the average number of particles A_S adsorbed on the substrate evolves (at long time) as $M'(t) \sim t/\ln t$.

There is a practical interest in understanding the spatial distribution of adsorbed particles in the steady state [30] and one can thus ask, *what is the region of the 2D substrate where one can find more A_S particles?*

To answer this question, from Eq. (63), we proceed as in Sec. IV B and, according to Eq. (40), we see that when α

$> \beta(\beta > \alpha)$, the region richer in A_S particles is outside (within) the disk Int $\mathcal{C}(c, R)$ [defined in Sec. IV B], where the concentration of A_S is $c_r(\infty) \geq \frac{1}{2}[c_r(\infty) \leq \frac{1}{2}]$. When $\alpha = \beta$, the 2D substrate is separated into two half-planes with concentration of $A_S > 1/2$ in the region including the origin.

VI. SUMMARY AND CONCLUSION

In this work we have shown how to compute some exact properties of a class of many-body stochastic systems in the presence of an arbitrary number of inhomogeneities n and have specifically focused on the voter model and monomer-monomer catalytic reaction (in the reaction-controlled limit). We have studied the effects of local perturbations of the dynamical rules on the static and time-dependent properties of these models by obtaining both general (yet formal) and many explicit results in the presence of one and two inhomogeneities. In fact, the latter situation already displays and covers most of the generic features of the models. Namely, when there is only one inhomogeneity present, it is responsible for a uniform and "unanimous" steady state in low dimensions [4], while in the presence of competing inhomogeneities ($n > 1$) the steady state is fluctuating and reactive. For the sake of concreteness we have mainly focused on the amenable case with two inhomogeneities and have shown quantitatively how the local interactions deeply affect the properties of these systems. Neither the stationary nor the time-dependent expression of the order parameters are translationally invariant but exhibit nontrivial radial and polar dependence (when $d > 1$).

From a sociophysical perspective, in voter model language, this means that a system which tolerates the presence of "competing zealots"—i.e., which accepts the competition between opposite points of view—will never reach a unanimous state but always end in a final configuration where both opinions coexist and fluctuate. Of course, such a conclusion seems to be consistent with the results of electoral competitions in modern democracies.

In the presence of competing inhomogeneities ($n > 1$) in low dimensions, subtle coarsening phenomena take place in 1D and 2D. In fact, the local and competing perturbations of the dynamics lead us to distinguish the case where the number of inhomogeneities is finite and the case where their number is comparable to the size of the system. In the former case the system coarsens and large domains develop, but their size are typically limited by the number of competing inhomogeneities, while in the latter case coarsening is prevented by the interaction with all the numerous inhomogeneities.

More specifically, in this work we have obtained exact, yet formal, expressions of the static and time-dependent order parameters [see Eqs. (15) and (50)]. The main technical problem to carry out detailed calculation resides in the inversion of the $n \times n$ matrix $\mathcal{N}$. The case with one single inhomogeneity in the voter model was already considered in [4] and here we show that such results can be translated in the language of the catalysis reaction. In particular we have shown that on 1D and 2D substrates, the presence of a single spatial inhomogeneity favoring the adsorption of one

species—say, A_S—with respect to the other is sufficient to ensure that eventually the substrate will be completely filled with A_S particles. When we have two competing inhomogeneities, favoring locally opposite states or the adsorption of particles of different species, we have obtained rich behavior. In 1D, between the two inhomogeneities, the stationary profiles of the order parameters vary linearly with the distance from the origin (22) and (58) and then reaches two plateaus (23), (24), (59), and (60). These static profiles are always reached algebraically in 1D: $S_r(t) - S_r(\infty) \simeq A t^{-1/2}$ and $c_r(t) - c_r(\infty) \simeq A' t^{-1/2}$, where the amplitudes A and A' depend nontrivially on all parameters of the problem and in particular on the separating distance between the inhomogeneities [see Eqs. (23), (24), (59), and (60)]. Far away from the inhomogeneities, the order parameters display scaling expression of the variable $r/\sqrt{t}$ [see Eqs. (25), (61), and (62)]. In one dimension, we have also been able to compute the expression of the stationary magnetization in the completely disordered situation where the number of zealots is arbitrary large [see Eqs. (27)–(33)]. In two dimensions, for $n = 2$, in the presence of two competing inhomogeneities, we have obtained non-uniform and nontrivial stationary profiles for the order parameters, in agreement with an electrostaticlike reformulation, the latter display logarithmic spatial dependence (radial and polar) [Eqs. (37) and (63)]. The approach toward the reactive steady state is very slow: $S_r(t) - S_r(\infty) \simeq B/\ln t$ and $c_r(t) - c_r(\infty) \simeq B'/\ln t$, with amplitudes B and B' depending again nontrivially on all parameters of the problem [see Eqs. (39) and (64)]. In 2D, for the inhomogeneous voter model, we have also studied the spatial regions with positive and negative static magnetization and have shown that only within a circle, whose center and radius depend on the strength of the "zealots" and on the distance between the latter, the sign of the magnetization is the one favorite by the "weakest" zealot. When both zealots have the same strength, there is positive and negative magnetization in half-space. In three dimensions, for $n = 2$ and in the continuum limit, we have shown that the stationary magnetization of the inhomogeneous voter model displays a radial and polar dependence that can be recast into a multipole expansion (44), corresponding formally to the electrostatic potential generated by two "charges" that are determined self-consistently using exact results from the discrete lattice system. The connection with electrostatics is particularly striking in the limit where both zealots have an infinite strength; thus, the stationary magnetization corresponds to the potential of an electric dipole. The approach toward the static magnetization follows a power law $S_r(t) - S_r(\infty) \simeq C t^{-1/2}$ [see Eq. (46)]. Also, in 3D we have studied the spatial regions with positive and negative magnetization and have shown that outside from a sphere whose center and radius depend on the parameters of the system and varies linearly with the distance separating the zealots, the sign of the final magnetization is the one favored by the strongest zealot.

The results obtained from Monte Carlo simulations of one- and two-dimensional lattices show excellent agreement with the theoretical results obtained for an infinite system. In the presence of multiple ($n > 2$) competing inhomogeneities the calculations in two dimensions become very tedious and

we consider this case by numerical simulations which confirm the extremely slow dynamics and the existence of nontrivial spatial dependence of the order parameters. We also would like to point out one intriguing and interesting fact about the small-time behavior of the magnetization of the zealots in the one-dimensional case. As it can be extracted from Fig. 3, $S_0(t)$ and $S_x(t)$, for small t, evolve as a power law with an exponent numerically smaller than 0.50. The small-time behavior of the site magnetization of the usual one-dimensional voter model (no inhomogeneities) is linear—i.e., $S_r(t) - S_r(0) \propto t$ for any site r on the lattice. We think it would be interesting to investigate further this "anomalous" small-t behavior of the magnetizations of the zealots in the one- and two-dimensional cases and we plan to do it in our future work. Various generalizations of this work could also be investigated. For instance, it would be worthwhile to consider that the inhomogeneities would not be fixed but spatially distributed according to some function $\mathcal{P}(\{a^j\})$. In this case, one should also average on the quenched disorder (on the samples) and one would have to compute: $\bar{S}_r(t) \propto \Sigma_{\{a^j\}} \mathcal{P}(\{a^j\}) S_r(\{a^j\}, t)$, where $S_r(\{a^j\}, t)$ is the quantity studied in this work for a given set of inhomogeneities at sites $\{a^j\}$. In the same manner, it would be quite interesting to consider the disordered case where the strength of the inhomogeneities would follow a distribution function such as $\widetilde{\mathcal{P}}(\{\alpha_j\}) \propto \Pi_{j=1}^n e^{-(\alpha_j - \bar{\alpha})^2/2\sigma}$. In this case, one would be interested in the quantity:

$$\widetilde{S}_r(t) = \int \prod_j d\alpha_j \widetilde{\mathcal{P}}(\{\alpha_j\}) S_r(\{a^j\}, \{\alpha^j\}, t),$$

where $S_r(\{a^j\}, \{\alpha^j\}, t)$ is the magnetization computed in this work for a given set of inhomogeneities at sites $\{a^j\}$, with strength $\{\alpha^j\}$.

[1] *Nonequilibrium Statistical Mechanics in One Dimension*, edited by V. Privman (Cambridge University Press, Cambridge, England, 1997); D. ben-Avraham and S. Havlin, *Diffusion and Reactions in Fractals and Disordered Systems* (Cambridge University Press, Cambridge, England, 2000); S. Redner, *A Guide to First-passage Processes* (Cambridge University Press, Cambridge, England, 2001); M. Henkel, E. Orlandini, and J. Santos, Ann. Phys. (N.Y.) **259**, 163 (1997); D. C. Mattis and M. L. Glasser, Rev. Mod. Phys. **70**, 979 (1998).

[2] F. Spitzer, Adv. Phys. **5**, 246 (1970); T. M. Liggett, *Interacting Particles Systems* (Springer, New York, 1985).

[3] A. J. Bray, Adv. Phys. **43**, 357 (1994); J. Duran and R. Jullien, Phys. Rev. Lett. **80**, 3547 (1998) S. N. Majumdar, D. S. Dean, and P. Grassberger, *ibid.* **86**, 2301 (2001); E. Ben-Naim and P. L. Krapivsky, Eur. Phys. J. E **8**, 507 (2002).

[4] M. Mobilia, Phys. Rev. Lett. **91**, 028701 (2003).

[5] P. L. Krapivsky, Phys. Rev. A **45**, 1067 (1992); J. Phys. A **25**, 5831 (1992).

[6] L. Frachebourg and P. L. Krapivsky, Phys. Rev. E **53**, R3009 (1996).

[7] E. Ben-Naim, L. Frachebourg, and P. L. Krapivsky, Phys. Rev. E **53**, 3078 (1996).

[8] I. Dornic, H. Chaté, J. Chavé, and H. Hinrichsen, Phys. Rev. Lett. **87**, 045701 (2001).

[9] F. Vazquez, P. L. Krapivsky, and S. Redner, J. Phys. A **36**, L61 (2003).

[10] D. Vilone and C. Castellano, Phys. Rev. E **69**, 016109 (2004).

[11] S. Galam, Y. Gelfen, and Y. Shapir, Math. J. Sociol. **9**, 1 (1982); S. Galam and S. Moscovici, Eur. J. Social Psychol. **21**, 49 (1991).

[12] P. L. Krapivsky and S. Redner, Phys. Rev. Lett. **90**, 238701 (2003); M. Mobilia and S. Redner, Phys. Rev. E **68**, 046106 (2003).

[13] S. Galam, Eur. Phys. J. B **25**, 403 (2002); e-print cond-mat/0307404.

[14] K. Sznajd-Weron and J. Sznajd, Int. J. Mod. Phys. C **11**, 1157 (2000).

[15] F. Slanina and H. Lavicka, Eur. Phys. J. B **35**, 279 (2003).

[16] C. J. Tessone, R. Toral, P. Amengual, H. S. Wio, and M. San-Miguel, e-print cond-mat/0403339; K. Suchecki, V. M. Eguiluz, and M. San Miguel, e-print cond-mat/0408101; K. Klemm, V. M. Eguiluz, R. Toral, and M. San Miguel, Phys. Rev. E **67**, 045101(R) (2003); C. Castellano, M. Marsili, and A. Vespignani, Phys. Rev. Lett. **85**, 3536 (2000).

[17] R. J. Glauber, J. Math. Phys. **4**, 294 (1963).

[18] G. Forgacs, D. Mukamel, and R. A. Pelcovits, Phys. Rev. B **30**, 205 (1984).

[19] M. Boudart and G. Djega-Mariadassou, *Kinetics of Heterogeneous Catalytic Reactions* (Princeton University Press, Princeton, 1984).

[20] *Handbook of Mathematical Functions*, edited by M. Abramowitz and I. Stegun (Dover, New York, 1965); I. S. Gradshteyn and I. M. Ryzhik, *Table of Integrals, Series and Products* (Academic Press, San Diego, 1963).

[21] *Tables of Integral Transforms*, edited by A. Erdélyi (McGraw-Hill, New York, 1954).

[22] M. L. Glasser and J. Boersma, J. Phys. A **33**, 5017 (2000).

[23] I. M. Campbell, *Catalysis at Surfaces* (Chapman and Hall, New York, 1988).

[24] R. M. Ziff and K. Fichthorn, Phys. Rev. B **34**, 2038 (1986); K. A. Fichthorn, R. M. Ziff and E. Gulari, in *Catalysis 1987*, edited by J. M. Ward (Elsevier, Amsterdam, 1988); P. Meakin and D. Scalapino, J. Chem. Phys. **87**, 731 (1987); K. Fichthorn, E. Gulari, and R. Ziff, Phys. Rev. Lett. **63**, 1527 (1989); D. ben-Avraham, D. Considine, P. Meakin, S. Redner, and H. Takayasu, J. Phys. A **23**, 4297 (1990); D. ben-Avraham, S.

Redner, D. Considine, and P. Meakin, *ibid.* **23**, L613 (1990).

[25] H. C. Kang and W. H. Weinberg, Phys. Rev. E **48**, 3464 (1993).

[26] H. C. Kang, W. H. Weinberg, and M. W. Deem, J. Chem. Phys. **93**, 6841 (1990); P. L. Krapivsky, Phys. Rev. E **52**, 3455 (1995).

[27] G. Yablonskii, V. Bykov, A. Gorban, and V. Elokhin, in *Comprehensive Chemical Kinetics*, edited by R. G. Compton (Elsevier, New York, 1991), Vol. 32.

[28] L. Frachebourg, P. L. Krapivsky, and S. Redner, Phys. Rev. Lett. **75**, 2891 (1995); D. A. Head and G. J. Rodgers, Phys. Rev. E **54**, 1101 (1996).

[29] G. Oshanin, M. N. Popescu, and S. Dietrich, Phys. Rev. Lett. **93**, 020602 (2004).

[30] M. D. Graham, M. Bär, I. G. Kevrekidis, K. Asakura, J. Lauterbach, H.-H. Rotermund, and G. Ertl, Phys. Rev. E **52**, 76 (1995).